CRYSTAL GROWTH & DESIGN

Article

pubs.acs.org/crystal

# Mechanistic Aspects for the Formation of Copper Dimer Bridged by Phosphonic Acid and Extending Its Dimensionality by Organic and Inorganic Linkers: Synthesis, Structural Characterization, Magnetic Properties, and Theoretical Studies

Bharat Kumar Tripuramallu,[†] Sandip Mukherjee,[‡] and Samar K. Das*[,†]

[†]School of Chemistry, University of Hyderabad, P.O. Central University, Hyderabad, 500046, India

[‡]Department of Inorganic and Physical Chemistry, Indian Institute of Science, Bangalore-560012, India

Supporting Information

**ABSTRACT:** Six new copper metal complexes with formulas $[Cu(H_2O)(2,2'\text{-bpy})(H_2L)]_2\cdot H_4L\cdot 4H_2O$ (**1**), $[\{Cu(H_2O)(2,2'\text{-bpy})(H_3L)\}_2(H_2L)]\cdot 2H_2O$ (**2**), $[Cu(H_2O)(1,10\text{-phen})(H_2L)]_2\cdot 6H_2O$ (**3**), $[Cu(2,2'\text{-bpy})(H_2L)]_n\cdot nH_2O$ (**4**), $[Cu(1,10\text{-phen})(H_2L)]_n\cdot 3nH_2O$ (**5**), and $[\{Cu(2,2'\text{-bpy})(MoO_3)\}_2(L)]_n\cdot 2nH_2O$ (**6**) have been synthesized starting from *p*-xylylenediphosphonic acid ($H_4L$) and 2,2′-bipyridine (2,2′-bpy) or 1,10-phenanthroline (1,10-phen) as secondary linkers and characterized by single crystal X-ray diffraction analysis, IR spectroscopy, and thermogravimetric (TG) analysis. All the complexes were synthesized by hydrothermal methods. A dinuclear motif (Cu-dimer) bridged by phosphonic acid represents a new class of simple building unit (SBU) in the construction of coordination architectures in metal phosphonate chemistry. The initial pH of the reaction mixture induced by the secondary linker plays an important role in the formation of the molecular phosphonates **1**, **2**, and **3**. Temperature dependent hydrothermal synthesis of the compounds **1**, **2**, and **3** reveals the mechanism of the self-assembly of the compounds based on the solubility of the phosphonic acid $H_4L$. Two-dimensional coordination polymers **4**, **5**, and **6**, which are formed by increasing the pH of the reaction mixture, comprise Cu-dimers as nodes, organic ($H_2L$) and inorganic ($Mo_4O_{12}$) ligands as linkers. The void space-areas, created by the (4,4) connected nets in compounds **4** and **5**, are occupied by lattice water molecules. Thus compounds **4** and **5** have the potential to accommodate guest species/molecules. Variable temperature magnetic studies of the compounds **3**, **4**, **5**, and **6** reveal the antiferromagnetic interactions between the two Cu(II) ions in the eight-membered ring, observed in their crystal structures. A density functional theory (DFT) calculation correlates the conformation of the Cu-dimer ring with the magnitude of the exchange parameter based on the torsion angle of the conformation.

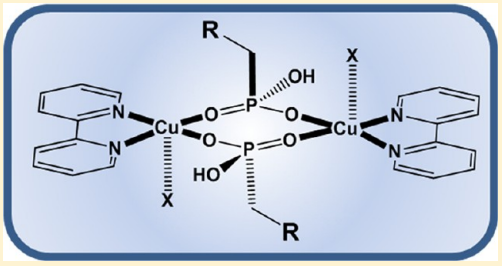


## INTRODUCTION

Over the past few decades, structural inorganic chemistry has provided a firm relationship between the aesthetics of crystalline architectures and their potential functions, in which the ultimate goal is to obtain the desired tailor-made materials with intriguing functional properties.[1] In order to model the functional crystalline solids with desired properties, considerable efforts have been devoted to understand the self-assembly process of the coordination networks.[2] In this context, numerous coordination polymers have been reported by utilizing the multitopic building blocks such as carboxylates,[3] phosphonates,[4] sulfonates,[5] organonitrogen bridging ligands and terminal aromatic chelating ligands,[6] etc. The majority of metal organic framework (MOF) structures rely on carboxylate derivatives, as the concerned bidentate ligands have regular coordination modes.[7] In contrast, metal organophosphonates are also among the earliest and extensively studied examples of coordination polymers/metal organic frameworks, that are important because of their potential applications in the areas of sorption, ion exchange, sensing, and catalysis.[8] Additionally, metal phosphonates have offered great opportunities to understand fundamental magnetic phenomena, such as spin canting, anisotropy, relaxation dynamics and field induced magnetic transitions.[9] Shimzu et al. reviewed the recent progress in phosphonate MOFs with an emphasis on open frameworks.[10] Because of availability of more possible ligating modes and three possible protonation states of $PO_3H_2$ groups, the controlled formation of geometrically well-defined structures has not succeeded. The self-assembly of metal phosphonate coordination polymers is dependent upon many factors, such as specific metal incorporation, degree of protonation, geometry of the phosphonic acid, and geometry of secondary linker as well as synthetic parameters under solvothermal conditions, e.g., temperature, pressure, vessel fill volume, time, pH, and the presence or absence of any mineralizing agent in the reaction mixture.[11] In order to

**Received:** August 3, 2012
**Revised:** August 31, 2012
**Published:** October 3, 2012

   dx.doi.org/10.1021/cg3011162 | *Cryst. Growth Des.* 2012, 12, 5579−5597

understand the structural consequences of some of the aforementioned factors, systematic studies are needed to evaluate the basic principles in the mechanisms of the self-assembly process of metal phosphonates. Our interests lie in the study of the factors that influence the self-assembly process of the coordination networks.[12] Recently, we discuss the factors affecting the conformational modulation of flexible ligands in the self-assembly process of coordination polymers of carboxylic acids.[13] Due to the availability of more number of ligating sites, phosphonic acids ($PO_3H_2$ groups) coordinate to more numbers of metal sites thereby forming a layered structure and the bisphosphonic acids form a pillared-layered structure.[14] Control over the protonation states and introduction of secondary chelating ligands result in the formation of clusters with different nuclearities.[15] This approach results in the stabilization of molecular phosphonates with interesting magnetic properties because the O−P−O bridge is known to be efficient in transmitting weak to moderately strong antiferromagnetic and ferromagnetic interactions.[16] In the recent era, research progress on metal phosphonates led to the evolution of two- and three-dimensional (2D and 3D) coordination networks.[17] In these extended networks, metal clusters act as nodes and organic parts act as linkers similar to carboxylic acids.[17e] Generally, the growth of single crystals with phosphonates is difficult as they often precipitate rapidly (as less ordered insoluble phases). Hydro(solvo)thermal techniques have been extensively employed in the synthesis of metal phosphonates to overcome this problem that hinders the formation of crystalline solids.[18] The investigation of the self-assembly process under the hydrothermal conditions by varying synthetic parameters reveals the mechanism of the formation of the crystalline solids. Among molecular phosphonates, two copper atoms connected by O−P−O bridges forming an eight-membered ring represent the simplest dinuclear model. On the basis of the torsion angles in the eight-membered ring, 10 symmetrical conformations have been established.[19] The magnetic exchange interactions in this dinuclear copper complex were reported with different peripheral subunits, but still it can be considered as a rare subunit to extend its dimensionality.[20] In this contribution, we have chosen *p*-xylylenediphosphonic acid ($H_4L$) as a organic linker and 2,2′-bpy or 1,10-phen as chelated secondary linkers with copper metal to construct the dinuclear copper systems. Recently we have reported both *cis* and *trans* conformations of the flexible *p*-xylylenediphosphonic acid with cobalt ion.[4g] Copper(II) compounds are of particularly interest from the theoretical point of view because they are the simplest paradigms of magnetic interactions that involve only two unpaired electrons.[21] Here we present syntheses and structural characterizations of six dinuclear copper complexes $[Cu(H_2O)(2,2'\text{-bpy})(H_2L)]_2\cdot H_4L\cdot 4H_2O$ (**1**), $[\{Cu(H_2O)(2,2'\text{-bpy})(H_3L)\}_2(H_2L)]\cdot 2H_2O$ (**2**), $[Cu(H_2O)(1,10\text{-phen})(H_2L)]_2\cdot 6H_2O$ (**3**), $[Cu(2,2'\text{-bpy})(H_2L)]_n\cdot nH_2O$ (**4**), $[Cu(1,10\text{-phen})(H_2L)]_n\cdot 3nH_2O$ (**5**), and $[\{Cu(2,2'\text{-bpy})(MoO_3)\}_2(L)]_n\cdot 2nH_2O$ (**6**). The mechanism for the formation dinuclear copper complex by varying the secondary linker at variant temperatures has been studied under hydrothermal conditions. The dimensionality of the Cu-dimers has been extended to 2D polymers by employing the organic and inorganic linkers. Temperature dependent magnetic measurements have been performed and the magnitudes of the exchange interactions have been calculated in the dimers. The relevant results are compared with theoretical values, calculated by density functional theory (DFT). The reversible dehydration and rehydration of lattice water molecules have been studied on compounds **4** and **5** demonstrating the host−guest properties.

## EXPERIMENTAL SECTION

**Materials and Methods.** All the chemicals were received as reagent grade and used without any further purification. The ligand *p*-xylylenediphosphonic acid ($H_4L$) was prepared according to the literature procedure.[22] Elemental analyses were determined by a FLASH EA series 1112 CHNS analyzer. Infrared spectra of solid samples obtained as KBr pellets on a JASCO − 5300 FT−IR spectrophotometer. Thermogravimetric analyses were carried out on an STA 409 PC analyzer and corresponding masses were analyzed by QMS 403 C mass analyzer, under the flow of $N_2$ gas with a heating rate of 5 °C $min^{-1}$, in the temperature range of 30−1000 °C. Powder X-ray diffraction patterns were recorded on a Bruker D8-Advance diffractometer using graphite monochromated $CuK_{\alpha 1}$ (1.5406 Å) and $K_{\alpha 2}$ (1.54439 Å) radiations. Magnetic susceptibilities were measured in the temperature range 2−300 K on a Quantum Design VSM-SQUID. All the compounds were synthesized in 23 mL Teflon-lined stainless steel vessels (Thermocon, India).

The following computational methodology was used to calculate the exchange coupling constants in the reported complexes.[23] The phenomenological Heisenberg Hamiltonian $H = -\Sigma_{(i>j)}J_{ij}S_iS_j$ (where where $S_i$ and $S_j$ are the spin operators of the paramagnetic metal centers $i$ and $j$; and the $J_{ij}$ parameters are the exchange-coupling constants for the different pairwise interactions between the paramagnetic metal centers of the molecule) can be used to describe the exchange coupling between each pair of transition-metal ions present in the polynuclear complex to construct the full Hamiltonian matrix for the entire system.

To calculate the exchange coupling constants for any polynuclear complex with $n$ different exchange constants, at least the energy of $n$ + 1 spin configurations must be calculated. For example, in the case of the studied dinuclear complexes, the exchange coupling value $J$ can be obtained by taking into account the energy of two different spin distributions: triplet with $S$ = 1, and singlet with $S$ = 0.

The hybrid B3LYP functional[24] has been used in all calculations as implemented in the *Gaussian 03* package,[25−28] We have used the LanL2DZ basis set for Cu atoms and 6-31g(d) basis set for the lighter atoms.[29] The calculations were performed on the complexes built from the experimental geometries.

**Synthesis of $[Cu(H_2O)(2,2'\text{-bpy})(H_2L)]_2\cdot H_4L\cdot 4H_2O$ (1) and $[\{Cu(H_2O)(2,2'\text{-bpy})(H_3L)\}_2(H_2L)]\cdot 2H_2O$ (2).** Compounds **1** and **2** are isolated from the same reaction mixture. To the mixture of $CuSO_4\cdot 5H_2O$ (0.087 g, 0.349 mmol), 2,2′-bpy (0.051 g, 0.320 mmol), and $H_4L$ (0.109 g, 0.407 mmol), 10.0 mL of distilled water was added. The resulting reaction mixture was stirred for 3 h and transferred to 23 mL Teflon lined stainless steel vessels, sealed and heated at 150 °C for 72 h followed by cooling to room temperature over 48 h to obtain blue color needle shaped crystals of **1** and blue block crystals of **2** in the same reaction mixture. (Initial and final pH values are 1.9 and 2.1.) Yield: ∼10% for **1** and 40% for **2** (based on Cu) Anal. Calcd. for $C_{44}H_{60}Cu_2N_4O_{24}P_6$ (**1**): C, 39.38; H, 4.50; N, 4.17. Found: C, 39.22; H, 4.03; N, 3.98 Anal. Calcd. for $C_{44}H_{56}Cu_2N_4O_{22}P_6$ (**2**): C, 40.47; H, 4.32; N, 4.29. Found: C, 40.22; H, 4.05; N, 4.16. IR (KBr pellet, $cm^{-1}$) for compound **1**: 3414, 3250, 3423, 3059, 2341, 1660, 1604, 1510, 1473, 1448, 1267, 1143, 1033, 920, 765, 565, 420. IR (KBr pellet, $cm^{-1}$) for compound **2**: 3429, 2920, 1660, 1608, 1504, 1450, 1257, 1032, 765, 549, 470.

**Synthesis of $[Cu(H_2O)(1,10\text{-phen})(H_2L)]_2\cdot 6H_2O$ (3).** The above-mentioned synthetic procedure has been used to synthesize compound **3** using 1,10-phenanthroline (0.063 g, 0.318 mmol) instead of 2,2′-bpy to obtain blue block crystals (Initial and final pH values are 2.5 and 2.4. Yield: 65% (based on Cu). Anal. Calcd. for $C_{40}H_{52}Cu_2N_4O_{20}P_4$: C, 41.42; H, 4.51; N, 4.83. Found: C, 41.22; H, 4.02; N, 4.38. IR (KBr pellet, $cm^{-1}$): 3470, 3080, 2918, 2361, 1655, 1581, 1518, 1429, 1261, 1147, 1047, 939, 852, 723, 561, 474, 424.


dx.doi.org/10.1021/cg3011162 | *Cryst. Growth Des.* 2012, 12, 5579−5597

Table 1. Crystal Data and Structural Refinement Parameters for Compounds 1−6

| | 1 | 2 | 3 |
|---|---|---|---|
| empirical formula | $C_{44}H_{60}Cu_2N_4O_{24}P_6$ | $C_{44}H_{56}Cu_2N_4O_{22}P_6$ | $C_{40}H_{52}CuN_4O_{20}P_4$ |
| formula weight | 1341.86 | 1305.83 | 1159.82 |
| $T$(K)/$\lambda$(Å) | 298(2) /0.71073 | 298(2) /0.71073 | 298(2) /0.71073 |
| crystal system | triclinic | monoclinic | triclinic |
| space group | $P\bar{1}$ | $P2_1/n$ | $P\bar{1}$ |
| $a$ (Å) | 7.506(4) | 9.9084(17) | 7.4340(8) |
| $b$ (Å) | 11.972(7) | 17.024(3) | 11.6079(13) |
| $c$ (Å) | 15.631(9) | 16.134(3) | 13.8609(16) |
| $\alpha$ (°) | 86.158(10) | 90 | 99.406(2) |
| $\beta$ (°) | 79.073(10) | 106.403(2) | 92.522(2) |
| $\gamma$ (°) | 81.553(10) | 90 | 97.815(2) |
| volume (Å$^3$) | 1363.1(13) | 2610.7(8) | 1166.4(2) |
| $Z$, $\rho_{calcd}$ (g cm$^{-3}$) | 1, 1.635 | 2, 1.661 | 1, 1.651 |
| $\mu$ (mm$^{-1}$), $F$(000) | 1.043, 692 | 1.084, 1344 | 1.134, 598 |
| goodness-of-fit on F$^2$ | 1.052 | 1.029 | 1.048 |
| $R_1/wR_2$ [$I > 2\sigma(I)$] | 0.0533/0.1170 | 0.0322/0.0895 | 0.0296/0.0832 |
| $R_1/wR_2$ (all data) | 0.0701/0.1252 | 0.0347/0.0913 | 0.0316/0.0847 |
| largest diff peak/hole (e Å$^{-3}$) | 0.567/−0.409 | 0.471/−0.568 | 0.423/−0.250 |
| | **4** | **5** | **6** |
| empirical formula | $C_{18}H_{20}CuN_2O_7P_2$ | $C_{20}H_{24}CuN_2O_9P_2$ | $C_{28}H_{28}Cu_2Mo_2N_4O_{14}P_2$ |
| formula weight | 501.84 | 561.89 | 1025.46 |
| $T$(K)/$\lambda$(Å) | 298(2)/0.71073 | 298(2)/0.71073 | 298(2)/0.71073 |
| crystal system | triclinic | triclinic | triclinic |
| space group | $P\bar{1}$ | $P\bar{1}$ | $P\bar{1}$ |
| $a$ (Å) | 9.9763(11) | 10.725(4) | 11.130(6) |
| $b$ (Å) | 10.1710(11) | 10.896(4) | 12.406(7) |
| $c$ (Å) | 11.3001(13) | 11.456(4) | 13.926(7) |
| $\alpha$ (°) | 110.125(2) | 66.984(6) | 71.952(8) |
| $\beta$ (°) | 108.317(2) | 64.714(5) | 72.257(8) |
| $\gamma$ (°) | 92.168(2) | 84.486(6) | 64.876(7) |
| volume (Å$^3$) | 1008.26(19) | 1110.1(7) | 1621.5(15) |
| $Z$, $\rho_{calcd}$ (g cm$^{-3}$) | 2, 1.653 | 2, 1.681 | 2, 2.100 |
| $\mu$ (mm$^{-1}$), $F$(000) | 1.287, 514 | 1.185, 578 | 2.227, 1016 |
| goodness-of-fit on F$^2$ | 1.047 | 1.056 | 1.065 |
| $R_1/wR_2$ [$I > 2\sigma(I)$] | 0.0342/0.0892 | 0.0607/0.1521 | 0.0291/0.0704 |
| $R_1/wR_2$ (all data) | 0.0420/0.0925 | 0.0786/0.1628 | 0.0333/0.0726 |
| largest diff peak/hole (e Å$^{-3}$) | 0.453/−0.374 | 1.737/−0.887 | 0.764/−0.475 |

**Synthesis of [Cu(2,2′-bpy)($H_2$L)]$_n$·$n$$H_2O$ (4).** A mixture of $CuSO_4$·5$H_2O$ (0.087 g, 0.349 mmol), $H_4$L (0.109 g, 0.407 mmol) and 2,2′-bpy (0.051 g, 0.320 mmol) was dissolved in 10.0 mL of distilled water. The pH of the reaction mixture was adjusted to 3.0 by addition of 5 M NaOH solution. Consequently the resulting mixture was stirred for 30 min and transferred to a 23 mL Teflon-lined stainless steel vessels, which was sealed and heated at 180 °C for 72 h and the reaction system was cooled to room temperature over 48 h to obtain green colored block crystals. Yield: 49% (based on Cu) Anal. Calcd. for $C_{18}H_{20}CuN_2O_7$ $P_2$: C, 43.08; H, 4.01; N, 5.58. Found: C, 42.91; H, 3.22; N, 5.22 IR (KBr pellet, cm$^{-1}$): 3398, 2916, 2851, 1579, 1518, 1429, 1257, 1134, 1049, 939, 902, 854, 723, 553.

**Synthesis of [Cu(1,10-phen)($H_2$L)]$_n$·3$n$$H_2O$ (5).** The same synthetic procedure as that of compound **4** was used to synthesize compound **5** using 1,10-phenanthroline (0.063 g, 0.318 mmol) instead of 2,2′-bpy and the pH of the reaction mixture was maintained at 4.0. Yield: 69% (based on Cu) Anal. Calcd. for $C_{20}H_{24}CuN_2O_9P_2$: C, 42.75; H, 4.30; N, 4.98. Found: C, 42.40; H, 3.83; N, 4.84 IR (KBr pellet, cm$^{-1}$): 3470, 3080, 2918, 2361, 1655, 1581, 1518, 1429, 1261, 1147, 1047, 939, 852, 723, 561, 474, 424

**Synthesis of [{Cu(2,2′-bpy)($MoO_3$)}$_2$(L)]$_n$·2$n$$H_2O$ (6).** A mixture of $CuSO_4$·5$H_2O$ (0.087 g, 0.349 mmol), 2,2′-bpy (0.051 g, 0.320 mmol), $Na_2MoO_4$·2$H_2O$ (0.105 g, 0.438 mmol), $H_4$L (0.109 g, 0.407 mmol) and water (10.0 mL) was taken in a 23 mL Teflon lined stainless steel vessel, and the pH was adjusted to 6.10 by 5 M HCl. The resulting mixture was stirred at room temperature for 60 min and heated at 180 °C for 72 h followed by cooling to room temperature over 48 h to obtain green block crystals (52% yield based on Mo). Anal. Calcd. for $C_{28}H_{28}Cu_2Mo_2N_4O_{14}P_2$: C, 32.79; H, 2.75; N, 5.46. Found: C, 32.42; H, 2.42; N, 5.27 IR (KBr pellet, cm$^{-1}$): 3454, 1643, 1601, 1493, 1469, 1444, 1309, 1165, 1051, 976, 883, 763, 729, 652, 551, 488, 410.

**Single Crystal X-ray Structure Determination of the Compounds 1−6.** Single-crystals suitable for structural determination of all the compounds (**1−6**) were mounted on a three circle Bruker SMARTAPEX CCD area detector system under Mo−K$\alpha$ ($\lambda$ = 0.71073A) graphite monochromated X-ray beam, crystal to detector distance 60 mm, and a collimator of 0.5 mm. The scans were recorded with an $\omega$ scan width of 0.3°. Data reduction performed by SAINTPLUS,[30a] empirical absorption corrections using equivalent reflections performed by program SADABS,[30b] structure solution using SHELXS-97[30c] and full-matrix least-squares refinement using SHELXL-97[30d] for above compounds. All the non-hydrogen atoms were refined anisotropically. Hydrogen atoms on the C atoms were introduced on calculated positions and were included in the refinement riding on their respective parent atoms. Attempts to locate the hydrogen atoms for the solvent water molecules in the crystal structure of compounds through Fourier electron density failed. However, no attempts were made to fix these atoms on their parents. The hydrogen atoms on some of the P−OH groups in the compounds


dx.doi.org/10.1021/cg3011162 | Cryst. Growth Des. 2012, 12, 5579−5597

are fixed by the proper HFIX commands and some are located by the Fourier electron density map. The oxygen atoms O6 and O5 of the terminal $PO_3H$ groups in the compound **2** suffer a significant disorder problem and they have been split over two positions after fixing their occupancies to 0.5 for each oxygen atom. Crystal data and structure refinement parameters for all the compounds (**1**–**6**) are summarized in Table 1, and selected bond lengths, bond angles are presented in the section 5 in the Supporting Information.

## RESULTS AND DISCUSSION

**Synthesis.** The title compounds **1**–**6** were synthesized by a conventional hydrothermal technique. A systematic approach has been attempted by employing organic and inorganic ligands to understand the formation of Cu-dimer and extending its dimensionality. The reaction mixture of $CuSO_4{\cdot}5H_2O$ (0.349 mmol), 2,2′-bpy (0.320 mmol), $H_4L$ (0.109 g, 0.407 mmol) in the ratio 1.09:1:1.16 with pH 1.90 at 150 °C results in the formation of compounds **1** and **2** in the product mixture. The yield of compound **1** is very low compared to that of **2** in the product mixture. Both the compounds **1** and **2** have identical chemical composition as far stoichiometric is concerned. The importance of copper dimer formed in **1** and the ambiguity in the formation of two compounds in the same reaction mixture lead us to carry out further reactions to understand the mechanism. $H_4L$ can exist in different protonation states depending upon the pH of the reaction mixture (Scheme 1).

**Scheme 1**

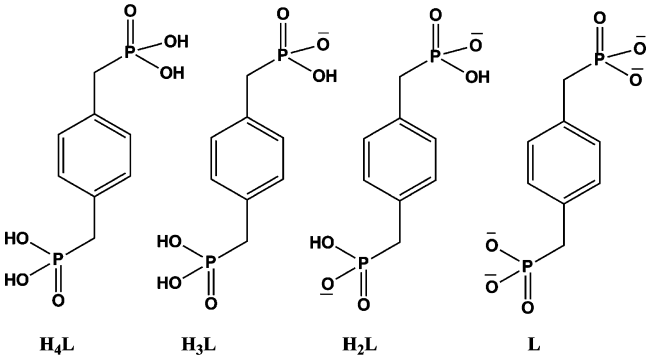


Different sets of reactions have been performed to obtain compound **1** as a major product in the product mixture. Initially, the temperature has been varied from 120 to 200 °C keeping concentration and time of reaction constant. At 120 °C, compound **1A** has been formed with composition $[Cu(2,2'\text{-bpy})(H_2O)_2(SO_4)]_n$, and in the temperature range 150–160 °C, we observe both the compounds **1** (minor product) and **2** (major product). The product mixture in this temperature range consists of blue needle shaped crystals of **1** and blue block crystals of **2** along with some unidentified blue powder. In the temperature range 160–200 °C, a pure crystalline form of compound **2** (in the form of large blue block crystals) was obtained. An attempt in obtaining compound **1** without neutral phosphonic acid ($H_4L$) as lattice component by decreasing the concentration of $H_4L$ in the relevant synthesis always results in the formation of **2** with low yield. By changing the concentration of the reactants and time of the reaction, the product mixture favors the formation of either **1A** or **2** in all the cases. The results indicate that compound **1** is thermodynamically less stable than compound **2**; the detailed mechanism is discussed in the later sections. In order to stabilize the Cu-dimer core in **1**, a different set of reactions was performed by changing the pH of the reaction mixture and adding secondary reactants. Because of different possible degrees of deprotonation, pH of the reaction mixture plays an important role in the self-assembly process. The presence of $H_4L$, $H_3L$, and $H_2L$ ligands (see Scheme 1) in the crystal structures of compounds **1** and **2** indicates the partial deprotonation of the ligand at the pH 1.90. Increasing the pH of the reaction mixture from 1.90 to 3.0 by adding 5 M NaOH and heating the reaction mixture at 180 °C results in the formation of 2D coordination polymer **4**. By adding sodium molybdate in the reaction mixture and adjusting the pH to 6.10 followed by heating the reaction mixture at 180 °C results in the 2D coordination polymer **6** with Cu-dimers extended by tetramolybdate subunits. Replacing the 2,2′-bpy with 1,10-phen in the reaction mixture, with initial pH 2.50 results in the formation of **3A** at 120 °C and **3** at 150 °C and with higher pH (4.0) at 180 °C affords a 2D coordination polymer **5**. The detailed synthesis has been described in Scheme 2.

**Description of Crystal Structures.** *$[Cu(2,2'\text{-bpy})(H_2O)_2(SO_4)]_n$ (**1A**) and $[Cu(1,10\text{-phen})(H_2O)_2(SO_4)]_n$ (**3A**).* Both the compounds $[Cu(2,2'\text{-bpy})(H_2O)_2(SO_4)]_n$ (**1A**) and $[Cu(1,10\text{-phen})(H_2O)_2(SO_4)]_n$ (**3A**) are isostructural and crystallize in monoclinic space group $C2/c$. Both the compounds are synthesized by heating the reaction mixture of $CuSO_4{\cdot}5H_2O$, 2,2′-bpy, or 1,10-phen, and $H_4L$ in the ratio 1.09:1:1.16 at pH 1.90 and heated at 120 °C for 72 h. These two compounds are obtained in the process of studying the

**Scheme 2**

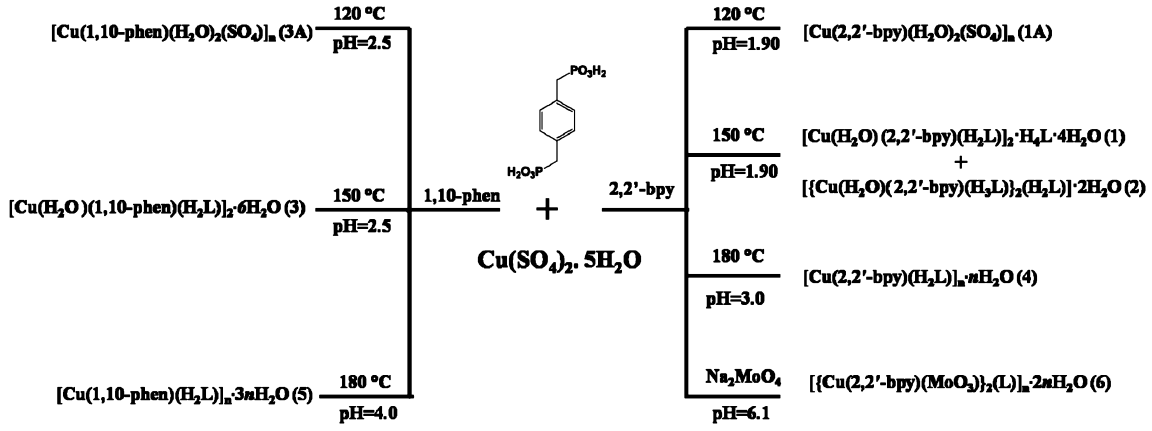



dx.doi.org/10.1021/cg3011162 | Cryst. Growth Des. 2012, 12, 5579–5597

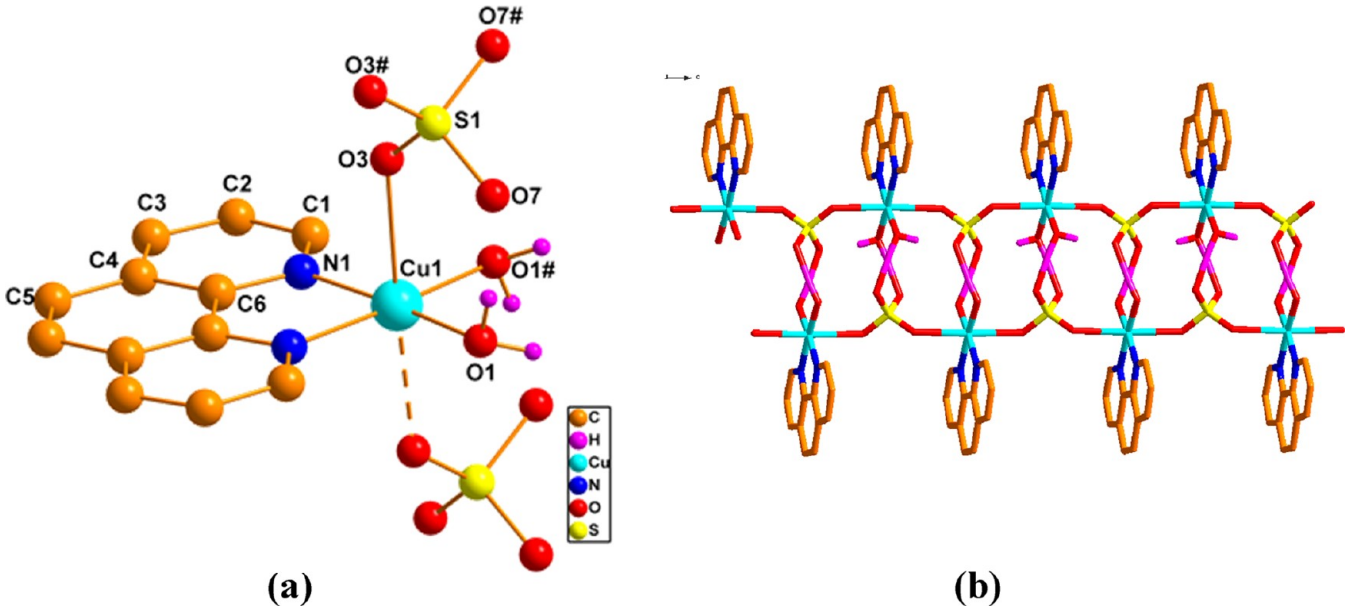


**Figure 1.** (a) Molecular diagram of the compound **3A**. (b) 1D tube formed through hydrogen bonding between two 1D chains by the coordinated aqua molecules.

mechanism of formation of Cu-dimers. The coordination environment of metal center in both the compounds is octahedral in which two equatorial sites are occupied by the nitrogen atoms of the 2,2′-bipyridine and 1,10-phenanthroline rings (respectively in **1A** and **3A**) and the remaining two sites are occupied by the water molecules, and the apical sites are occupied by the sulfate anion $[SO_4]^{2-}$ (Figure 1a). The sulfate anion coordinates to the another adjacent Cu(2,2′-bpy)$(H_2O)_2$ unit thereby forming a 1D coordination polymer. Two adjacent such chains are connected to each other by noncovalent interactions involving the coordinated water molecules and sulfate anions to form a 1D tube structure (Figure 1b). Compounds **1A** and **3A** are reported earlier in the literature.[31] Crystallographic details of these compounds **1A** and **3A** are presented in the Supporting Information.

*[Cu(H$_2$O)(2,2′-bpy)(H$_2$L)]$_2$·H$_4$L·4H$_2$O* (***1***). Compound **1** is a discrete copper dimer that crystallizes in triclinic space group $P\bar{1}$. The molecular structure consists of two square pyramidal copper(II) ions bridged by two phosphonate oxygens (O2,O4) from two $H_2L^{2-}$ ligands in the basal plane to form a dimer; the rest of the coordination sites of each copper ion in the basal plane are occupied by two nitrogen atoms from the 2,2′-bpy molecule. The apical position of each copper is accommodated by one aqua ligand. One neutral phosphonic acid ($H_4L$) and two water molecules remain in the lattice void per formula unit (Figure 2a). In the bridging region, one arm of each $H_2L$ bridges two Cu ions through P═O and P−O$^-$ groups to form a dimer leaving P−OH group in the interstitial position and the other arm remains uncoordinated to form a discrete compound. The distance between two copper metal centers in the dimer is 5.123 Å. The eight membered Cu-dimer can exist in 10 canonical conformations, among which the dimer formed in this crystal structure (compound **1**) is confined to a chair conformation. The assignment of P═O, P−O$^-$, and P−OH bonds are consistent with the literature.[32] Because of the relatively low acidic pH in the relevant reaction mixture, it results in the stabilization of $H_4L$ without deprotonation in the crystal lattice. All these lattice phosphonic acids are present in *trans* conformation with an antiperiplanar torsion angle of 180°. As anticipated, classical hydrogen bonding between the lattice phosphonic acid P−OH groups and the dimer phosphonic acid P−OH groups are observed with O···O separations varying from 2.474(4) to 3.024(6) Å. A 2D supramolecular network has been constructed by considering the interactions from the dimer in two directions. In this 2D arrangement, each dimer is linked to another dimer in the crystallographic *b* axis through the apical water molecule O1 and coordinated phosphonate oxygen atom O4 to form a ring $R^2_2(8)$ and extended to a one-dimensional chain. In another direction, each Cu-dimer is connected to another dimer through the P−OH groups of lattice $H_4L$ ligand, lattice aqua ligand O12, and phosphonate oxygen atom O6 of $H_2L$ in the crystallographic *a* axis to form a 10-membered ring $R^3_3(10)$. These two chains thread into each other to form a 2D supramolecular sheet as shown in Figure 3a. The main focus of the article deals with the formation and stability of the Cu-dimer mentioned and extending its dimensionality (vide infra).

*[{Cu(H$_2$O)(2,2′-bpy)(H$_3$L)}$_2$(H$_2$L)]·2H$_2$O* (***2***). Compound **2** is a discrete linear copper dimer that crystallizes in the monoclinic space group $P2_1/n$. The full molecule consists of two copper atoms chelated by two 2,2′-bpy rings coordinated to $H_3L$ ligands and linked by the phosphonate oxygen atoms of the $H_2L$ ligand. The square pyramidal geometry of each Cu(II) in the dimer is furnished by the two nitrogen atoms from the 2,2′-bpy ring, and two oxygen atoms (O10, O2) from the two different acid groups, one from the $H_2L$ and other from the $H_3L$ ligands respectively in the basal plane and one aqua ligand in the apical position. $H_2L$ ligand links two $\{Cu(H_2O)(2,2'\text{-bpy})(H_3L)\}^+$ groups by using P═O coordination to the metal center leaving two P−OH and P−O$^-$ groups in the interstitial positions, with both arms of the ligand (Figure 2b). $H_2L$ in the compound exists in $\mu_1$-$\eta_1$, $\eta_0$, $\eta_0$ coordination mode on both sides. In the same way two $H_3L$ ligands attached to the metal polyhedra through the P═O group with $\mu_1$-$\eta_1$, $\eta_0$, $\eta_0$ coordination mode through the $-PO_3H_2$ arm and the $-PO_3H$ arm on other side remains uncoordinated. The assignment of the P−OH, P−O$^-$, and P═O bonds for the different protonation states of the $H_4L$ are shown in Table 3,


dx.doi.org/10.1021/cg3011162 | *Cryst. Growth Des.* 2012, 12, 5579−5597

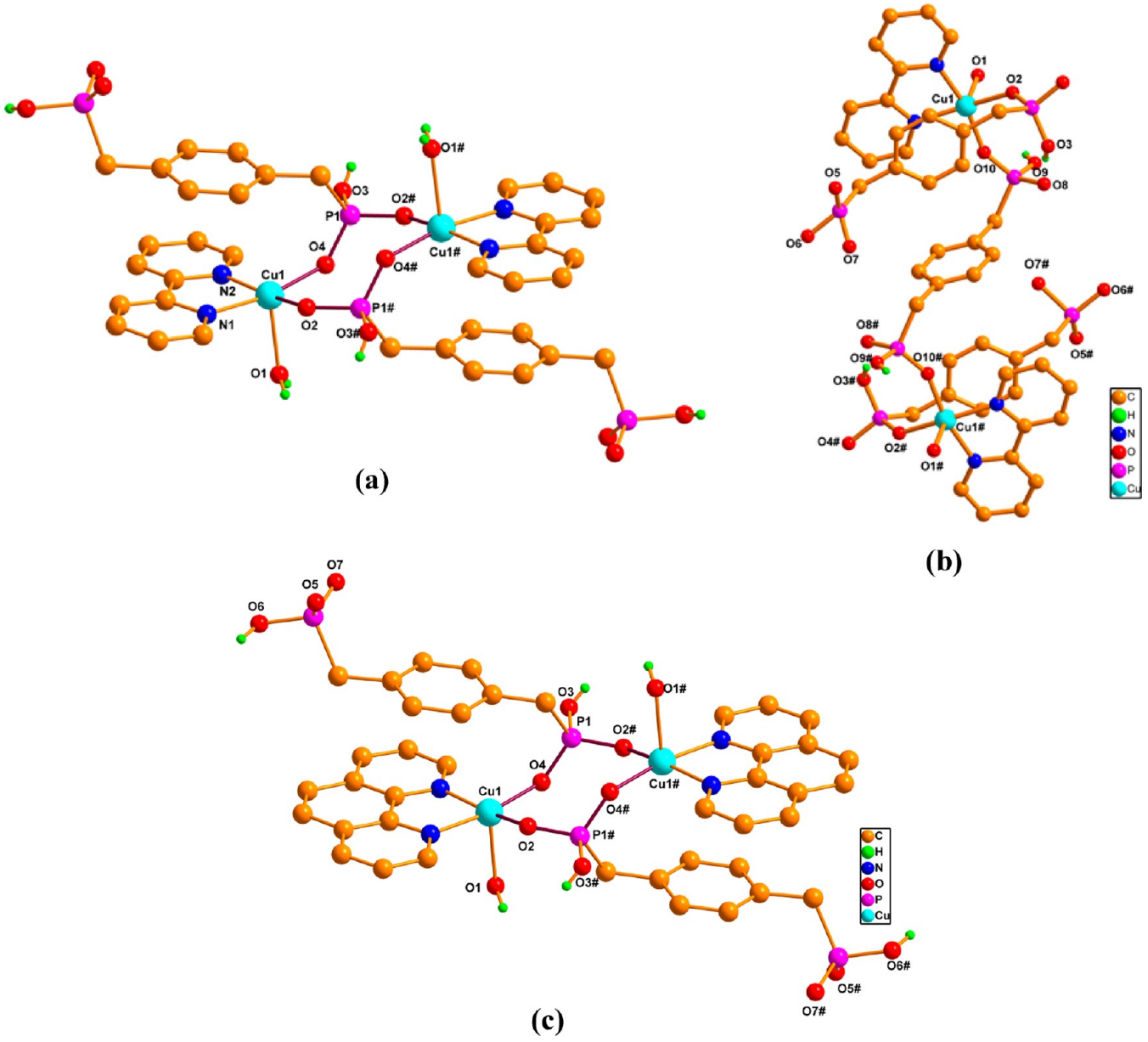


**Figure 2.** (a) Molecular diagram of the compound **1**; lattice $H_4L$ component has been removed for clarity. (b) Molecular diagram of compound **2**; (c) molecular diagram of compound **3**; hydrogen atoms on the carbon atoms and lattice water molecules are removed for the clarity in all the molecular diagrams.

that are consistent with the literature values.[32] A structural comparison between the compounds **1** and **2** reveals that compound **1** is an eight-membered dimer with $H_4L$ as a lattice component and **2** is a linear dimer and can be viewed as inclusion of lattice $H_4L$ to the coordination matrix as $H_2L$. The detailed mechanism for formation of these phases is discussed in the later section.

*$[Cu(H_2O)(1,10\text{-phen})(H_2L)]_2{\cdot}6H_2O$ (**3**).* Compound **3** is a discrete copper dimer, crystallized in triclinic space group $P\bar{1}$. The structure of copper dimer in compound **3** is same as that in compound **1** except that 2,2′-bipyridine is replaced by the 1,10-phenanthroline (Figure 2c). In compound **1** along with the dimer, a neutral $H_4L$ ligand also present in the crystal structure which is absent in the case of compound **3.** The transformation of Cu-dimer to the linear chain is not observed in the case of **3** probably due to the absence of $H_4L$ as a lattice component. Due to the presence of six lattice water molecules per formula unit of compound **3**, an extensive noncovalent interactions are observed in the crystal structure. The hydrogen bonding interactions between the lattice water molecules and the P−OH groups result in a 1D chainlike arrangement, and these chains with aid of the copper dimers form a 2D supramolecular network as shown in Figure 3b.

*$[Cu(2,2'\text{-bpy})(H_2L)]_n{\cdot}nH_2O$ (**4**).* Compound **4** is a two-dimensional coordination polymer constructed from the copper dimers and crystallizes in triclinic space group $P\bar{1}$. The relevant asymmetric unit consists of one copper metal center in square pyramidal geometry, chelated by 2,2′-bipyridine ring nitrogen atoms and coordinated to oxygen atoms of three different $H_2L$ ligands (Figure 4a). The structure of the copper dimer is the same as explained in compound **1** except the apical water molecule in the square pyramidal geometry is replaced by the oxygen atom of the $H_2L$ ligand in compound **4**. Compound **4** can be described as the uncoordinated phosphonate arm


dx.doi.org/10.1021/cg3011162 | *Cryst. Growth Des.* 2012, 12, 5579−5597

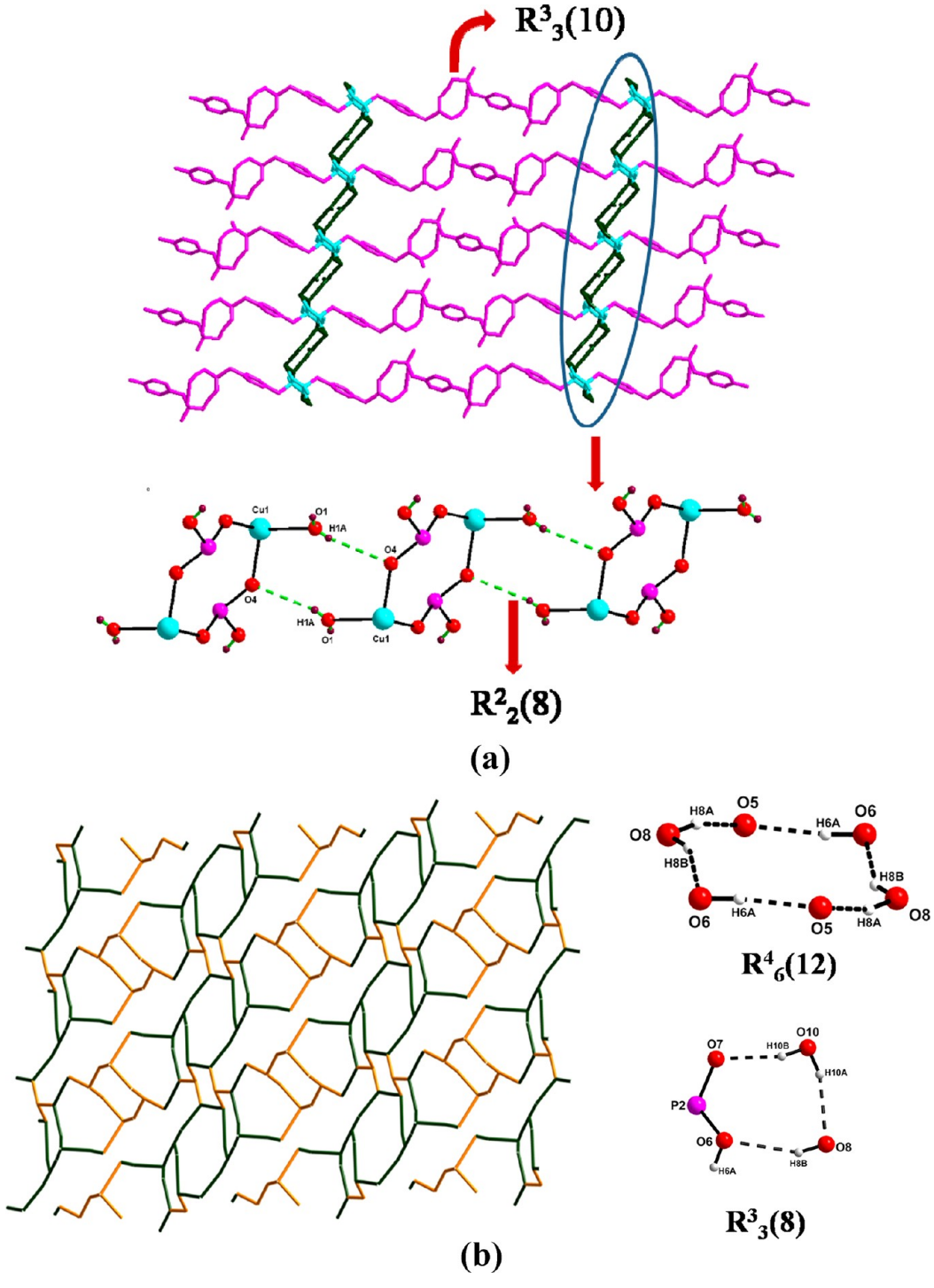


**Figure 3.** (a) 2D supramolecular network formed due to noncovalent interactions between the P−OH groups of lattice $H_4L$, coordinated $H_4L$ ligands and lattice aqua molecules in compound **1**. (b) 2D supramolecular network formed between six water molecules and P−OH groups of the coordinated $H_4L$ ligands in compound **3**.

(−$PO_3H$) of the copper dimer in compound **1** coordinated to another dimer in the $\mu_2$-$\eta_1$, $\eta_1$, $\eta_0$ coordination mode to form a one-dimensional chain constituted by Cu-dimers bridged by $H_2L$ ligands along the crystallographic *c* axis (Figure 4b). These chains are linked by another $H_2L$ ligand in $\mu_1$-$\eta_1$, $\eta_0$, $\eta_0$ coordination mode resulting in the formation of a 2D coordination polymer as shown in Figure 4c. In compound **4** two types of phosphonic acids which differ in the mode of the connectivity are involved; i.e., $\mu_2$-$H_2L$ bridges two Cu(II) ions to form 1D Cu-dimer chains and these chains are linked by the $\mu_1$-$H_2L$ ligand; the packing diagram of bridging and linking phosphonic acids is shown in Figure 4d. Topologically the structure can be viewed as (4, 4) connected net with Cu-dimers as vertices and $\mu_2$-$H_2L$, $\mu_1$-$H_2L$ as sides forming rectangular boxes with dimensions 11.73 × 11.30 Å, in which lattice water molecules are accommodated. Two lattice water molecules per one Cu-dimer are present in the crystal structure. These two lattice water molecules are situated in the middle of the


dx.doi.org/10.1021/cg3011162 | *Cryst. Growth Des.* 2012, 12, 5579−5597

**Table 2. Geometrical Parameters of the O−H···O Hydrogen Bonds (Å, °) Involved in Supramolecular Networks of Compounds 1, 3, 4, and 5[a]**

| D−H···A | d(D−H) | d(H···A) | d(D···A) | ∠(DHA) |
|---|---|---|---|---|
| compound **1** | | | | |
| O(14)−H(11C)···O(9)#3 | 0.76(5) | 0.23(5) | 2.964(5) | 161(5) |
| O(4)−H(9A)···O(5)#4 | 0.02(7) | 1.47(7) | 0.474(4) | 166(6) |
| O(10)−H(6A)···O(10)#5 | 0.85(6) | 1.66(6) | 2.511(5) | 171(6) |
| O(5)−H(1A)···O(4)#6 | 0.58(5) | 2.46(5) | 3.024(6) | 165(7) |
| O(3)−H(3A)···O(7)#7 | 0.74(4) | 1.85(5) | 2.584(4) | 172(5) |
| compound **3** | | | | |
| O(10)−H(10B)···O(7)#2 | 0.92(5) | 1.93(3) | 2.783(3) | 153(4) |
| O(10)−H(10A)···O(8)#3 | 0.86(4) | 2.12(4) | 2.928(7) | 156(3) |
| O(8)−H(8B)···O(6)#4 | 0.88(5) | 2.26(5) | 3.083(3) | 154(4) |
| O(8)−H(8A)···O(5)#5 | 0.95(5) | 1.91(5) | 2.825(3) | 163(4) |
| O(6)−H(6A)···O(5)#5 | 0.84(4) | 1.74(4) | 2.580(2) | 173(4) |
| O(3)−H(3A)···O(7)#6 | 0.70(3) | 1.89(3) | 2.580(2) | 173(3) |
| compound **4** | | | | |
| O(6)−H(6)···O(5)#4 | 0.82 | 1.78 | 2.598(3) | 174.2 |
| compound **5** | | | | |
| O(6)−H(6O)···O(5)#4 | 0.82 | 1.83 | 2.613(5) | 160.5 |
| O(7)−H(7B)···O(7)#5 | 0.72(12) | 2.21(11) | 2.859(15) | 132(15) |
| O(7)−H(7A)···O(6)#4 | 0.64(7) | 2.37(8) | 2.964(9) | 156(9) |
| O(9)−H(9B)···O(2)#6 | 0.94(11) | 2.35(11) | 3.199(8) | 150(9) |

[a]D = donor; A = acceptor. (**1**) #3 $-x, -y+1, -z+1$; #4 $-x+1, -y+2, -z+1$; #5 $-x, -y+2, -z+1$; #6 $-x, -y+1, -z$; #7 $-x+1, -y+2, -z$. (**3**) #2 $x, y-1, z$; #3 $-x+1, -y+1, -z+1$; #4 $-x+1, -y+2, -z+1$; #5 $-x, -y+2, -z+1$; #6 $-x, -y+2, -z+2$. (**4**) #4 $-x+1, -y+1, -z+1$. (5) #4 $-x+1, -y+1, -z+2$; #5 $-x, -y+1, -z+2$; #6 $x-1, y, z$.

**Table 3. Assignment of P−O Bond Lengths in the Compounds 1 and 2**

| coordination mode | compound **1** Cu-dimer (Å) | compound **2** linear Cu-chain (Å) |
|---|---|---|
| | **$H_2L$** | **$H_3L$** |
| P1−O2 | 1.500(P═O) | 1.517(P═O) |
| P1−O3 | 1.559(P−OH) | 1.528(P−OH) |
| P1−O4 | 1.510($P-O^-$) | 1.532(P−OH) |
| | **$H_2L$** | **$H_3L$** |
| P2−O5 | 1.513($P-O^-$) | |
| P2−O6 | 1.573(P−OH) | |
| P2−O7 | 1.496(P═O) | 1.474(P═O) |
| | **$H_4L$** | **$H_2L$** |
| P3−O8 | 1.546(P−OH) | 1.526($P-O^-$) |
| P3−O9 | 1.552(P−OH) | 1.556(P−OH) |
| P3−O10 | 1.483(P═O) | 1.492(P═O) |

rectangular box and exactly in the plane of 2D sheets. The distance between two layers viewed through the plane of phenyl group is 9.976 Å. Noncovalent interactions between the lattice water molecules (O7, O7#) of one layer to another layer are absent in the crystal structure. But the two layers are connected to each other with noncovalent interactions between the P−OH groups of the phosphonate arm in $\mu_1$-$H_2L$ ligand to form an eight-membered $R^2_2(8)$ ring thereby forming a 3D supramolecular network as shown in Figure 4e,f.

*[Cu(1,10-phen)($H_2L$)]$_n$·3n$H_2O$* (**5**). Compounds **4** and **5** are isostructural except 2,2′-bipyridine in compound **4** is replaced by 1,10-phenanthroline. Compound **5** also crystallizes in triclinic space group $P\bar{1}$ (Figure 5a). The coordination network and topological view of **5** are similar to those explained in compound **4**. The major difference between compounds **4** and **5** is the number of lattice water molecules and their arrangement in respective void spaces. In compound **5**, six water molecules per Cu-dimer are presented in the void spaces created by the (4,4) connected layers (Figure 5b). An intricate hydrogen bonded network is formed between the lattice water molecules and deprotonated P−OH groups of the layers. To explain this hydrogen bonding, we consider six lattice water molecules in the rectangular void as a single domain (O7, O8, O9, O9#, O8#, O7#). The intramolecular hydrogen bonding in the domains is constituted between four lattice water molecules O8, O9, O9#, and O8# to form short chains. These chains with terminus O8 and O8# are connected to remaining lattice water molecules O7 and O7# in the domain through the phosphonate oxygen atoms O5 and O6 of the layer to form a long chain (Figure 5c). The long chains of the adjacent domains are connected to each other to form a one-dimensional chain running through the crystallographic *c* axis. When viewed through the crystallographic *b* axis, the distance between two domains of different layers is 10.89 Å. Total number of lattice water molecules for one Cu-dimer is the same in both discrete compound **3** and 2D coordination polymer **5**. As mentioned in compound **4**, noncovalent interactions between the lattice water molecules of the two layers are absent, due to the large separation between the layers. But these layers are connected by the P−OH groups of the phosphonate arm in $\mu_1$-$H_2L$ ligand to form an eight-membered $R^2_2(8)$ ring resulting in the formation of a 3D supramolecular network.

*[{Cu(2,2′-bpy)($MoO_3$)}$_2$(L)]$_n$·2n$H_2O$* (**6**). Compound **6** is a 2D coordination polymer constructed from the Cu dimers bridged by the ligand L and linked by $Mo_4O_{12}$ subunits. The asymmetric unit consists of two copper atoms chelated by two 2,2′-bipyridine rings, $Mo_2O_3$ subunit, one ligand $L^{4-}$ bridging the Cu atoms and $Mo_2O_3$ subunit, and one lattice water molecule (Figure 6a). The ligand $H_4L$ is completely deprotonated and the three oxygen atoms of the each arm ($-CH_2-PO_3^{2-}$) connected to metal centers in $\mu_3$−$\eta_1$, $\eta_1$, $\eta_1$ bridging mode in which two oxygen atoms bridge two Cu metal centers and the remaining one oxygen atom connected to the Mo metal center. Two $L^{4-}$ ligands bridges the two Cu metal centers to form an eight-membered ring, and these rings are extended through the *p*-xylyl linkers to form a 1D Cu-dimer chain as shown in Figure 6b. These 1D chains are linked by the inorganic linker $Mo_4O_{12}$ to form a (4,4) connected 2D coordination polymer as shown in Figure 6c, unlike in compounds **4** and **5**, in which 1D chains are linked by organic linker $H_2L$. $Mo_4O_{12}$ subunit comprises edge sharing two $MoO_6$ and two $MoO_5$ polyhedra with four $\mu_2$-bridging oxygen atoms and eight terminal oxygen atoms (Figure 6d). Each $Mo_4O_{12}$ subunit is connected to two Cu-dimers from the opposite 1D chains by coordinating to the apical site of the Cu−metal polyhedra through terminal oxygen atoms with a separation of 12.54 Å between the two 1D chains. Also the oxygen atom which remains left in the phosphonate group after forming the Cu-dimer is coordinated to the Mo−polyhedra. The $\mu_3$ coordination of the phosphonate groups apart from the classical $\mu_2$ coordination (which was observed in the compounds **1**, **3**, **4**, and **5**) results in the crown conformation of the eight-membered ring apart from the chair conformation. The neutral tetramolybdate is sandwiched between the two 1D


dx.doi.org/10.1021/cg3011162 | Cryst. Growth Des. 2012, 12, 5579−5597

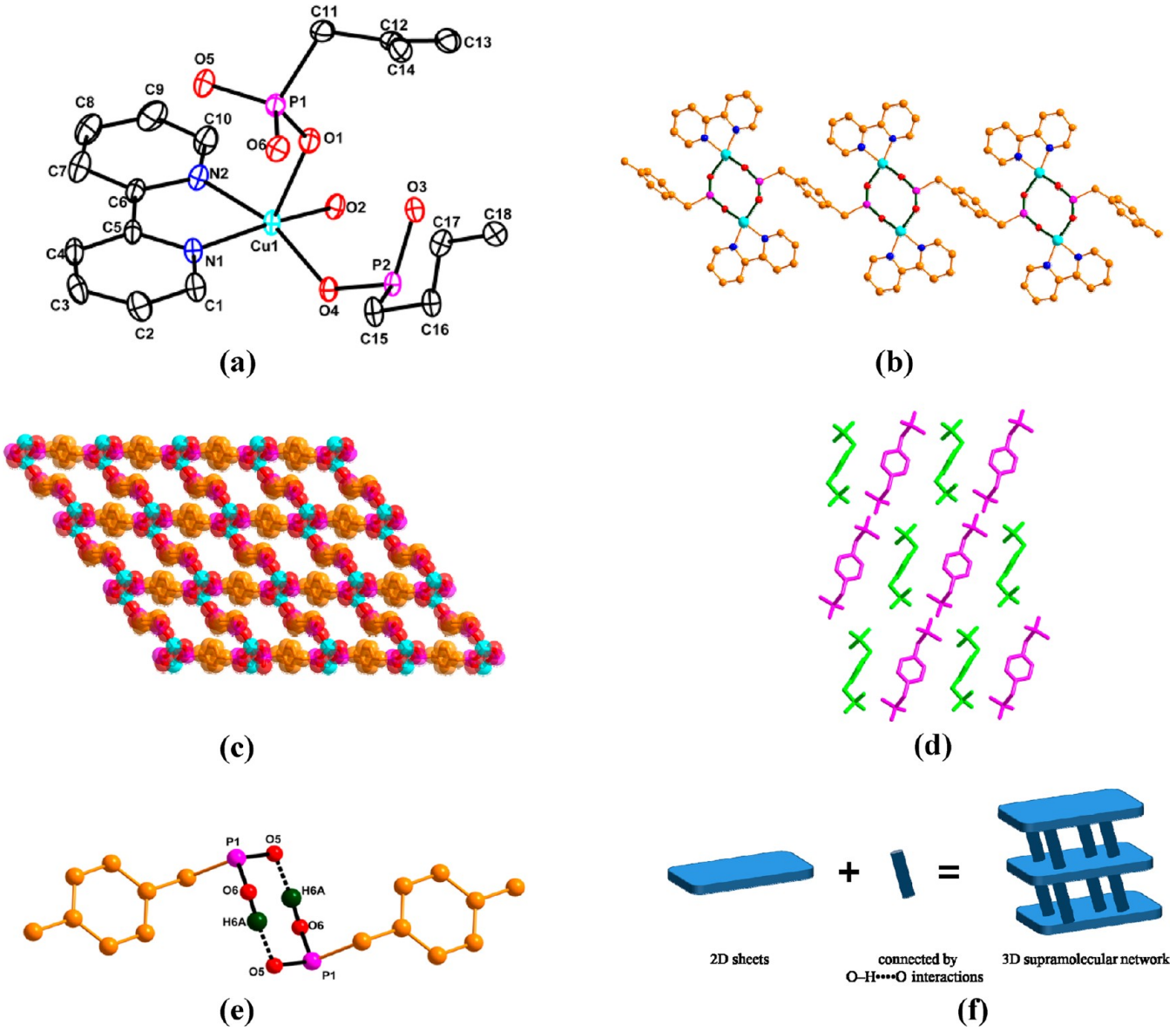


**Figure 4.** (a) ORTEP view of the basic unit of **4**. Hydrogen atoms and lattice water molecules have been removed for clarity. Thermal ellipsoids are at the 30% probability level. (b) One dimensional Cu-dimer chain running along the crystallographic *c* axis. (c) (4,4) connected 2D coordination polymer of **4**; lattice water molecules in the void space are removed for clarity. (d) Packing diagram of the linking and bridging phosphonic acids; green color represents bridging ligands and purple color represents linking ligands. (e) Noncovalent interactions connecting the two layers. (f) Scheme representing the formation of 3D supramolecular network from the 2D sheets through O−H···O interactions.

Cu-dimer chains with Cu−O and Mo−O bonds as pillars to form a 2D coordination polymer as shown in Figure 6e. Two lattice water molecules per Cu-dimer are located in the void spaces of the (4,4) connected network. Jubieta et al. reported a 3D compound $[\{Cu(bpy)\}_2Mo_4O_{10}(O_3PCH_2C_6H_4CH_2PO_3)_2]$ starting from the molybdenum oxide in which $\{Mo_4O_{10}(O_3PR)_4\}_n^{4n-}$ chains decorated with $\{Cu(bpy)\}^{2+}$ subunits and linked through the *p*-xylyl tethers of the diphosphonate ligand into a framework architecture.[33]

**Understanding the Formation of Copper Dimer and Extending Its Dimensionality by Organic and Inorganic Linkers.** As discussed in the section of synthesis, the serendipitous identification of compound **1** as a minor product along with compound **2** has prompted us to study the mechanism of formation of the dimer and its stability in the coordination matrix. Temperature plays an important role in the nucleation process under hydrothermal conditions. In the reaction mixture of $CuSO_4{\cdot}5H_2O$, 2,2′-bpy, and $H_4L$, copper sulfate pentahydrate remains presumably in the form of $[Cu(H_2O)_n]^{2+}$ counter balanced by a sulfate anion. At low temperature, the 2,2′-bipyridine ligand chelates the Cu metal center to form a $[Cu(2,2'\text{-bpy})(H_2O)_{n-2}]^{2+}$ complex by replacing the two water molecules in the equatorial positions. The apical water molecules of the Cu metal polyhedron are replaced by the sulfate anion to form a 1D coordination polymer $[Cu(2,2'\text{-bpy})(H_2O)_2(SO_4)]_n$ (**1A**). Because of the 1:1 ratio of $CuSO_4{\cdot}5H_2O$ and 2,2′-bpy, only two equatorial coordination sites are chelated by the bipyridine ring. The nonparticipation of the $H_4L$ in the complex **1A** is probably due to low solubility of phosphonic acid at a low temperature. As the temperature increases the solubility of the phosphonic acid increases and participates in the nucleation process and in the


dx.doi.org/10.1021/cg3011162 | *Cryst. Growth Des.* 2012, 12, 5579−5597

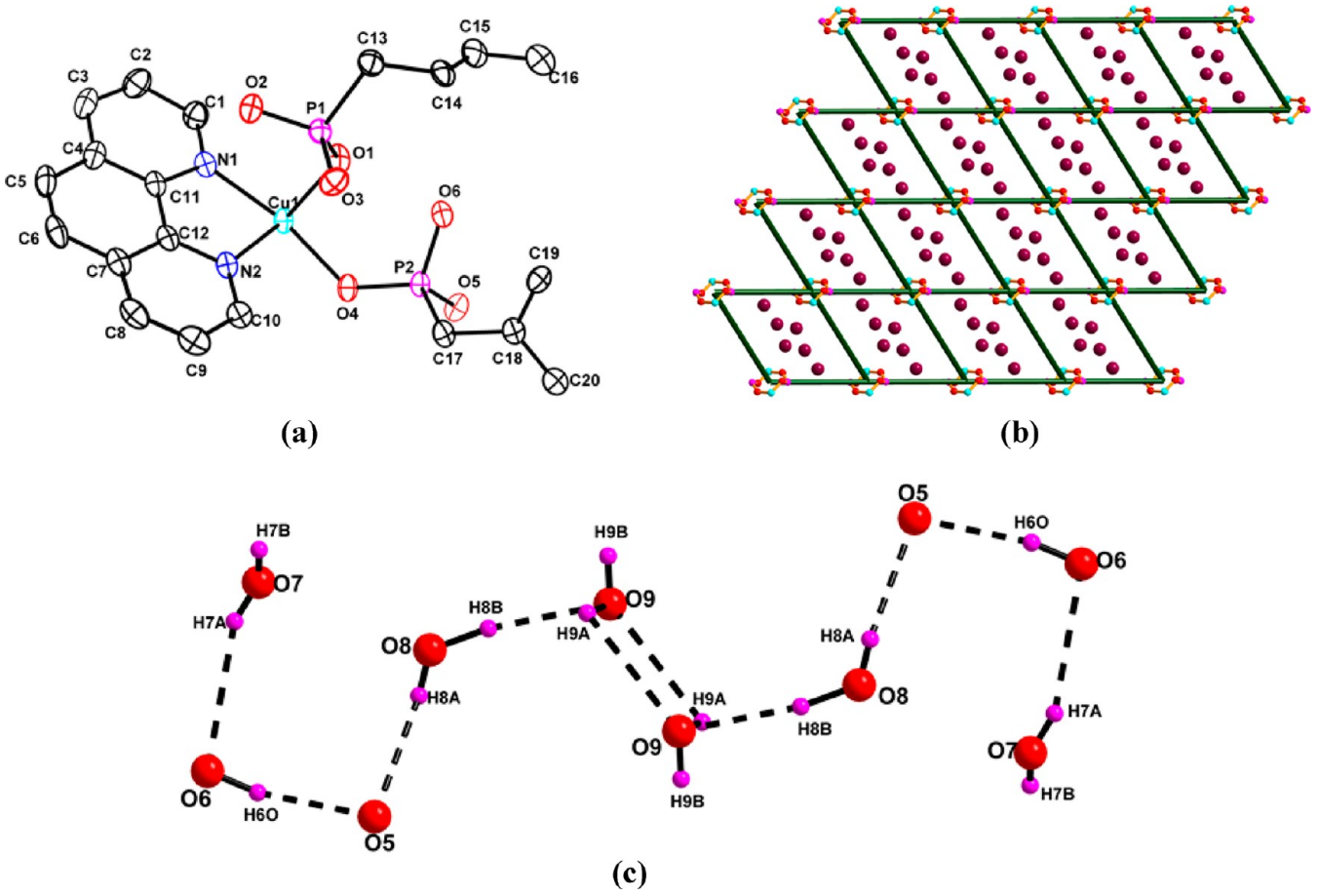


**Figure 5.** (a) ORTEP view of the basic unit of **5**. Hydrogen atoms and lattice water molecules have been removed for clarity. Thermal ellipsoids are at the 30% probability level. (b) (4,4) connected 2D coordination polymer of **5** representing the dimers as nodes and $H_2L$ ligands as linkers and lattice water molecules in the void space. (c) Noncovalent interactions between the lattice water molecules and phosphonate oxygen atoms in the single layer.

temperature region 150−160 °C, it gives two compounds **1** and **2**, among which in compound **1** phosphonic acid ($H_2L$) bridges the two $[Cu(2,2'\text{-bpy})]^{2+}$ units to form a dimer $[Cu(H_2O)(2,2'\text{-bpy})(H_2L)]_2$ (**1**) along with one neutral $H_4L$ ligand as a lattice component. In compound **2**, $H_2L$ links two $[Cu(2,2'\text{-bpy})(H_3L)]^{1+}$ units to form a linear chain of composition $[\{Cu(H_2O)(2,2'\text{-bpy})(H_3L)\}_2(H_2L)]\cdot 2H_2O$ (**2**). The yield of the dimeric compound **1** is very less in comparison to compound **2**. The attempts to isolate the compound **1** as a single product were unsuccessful, even by varying all the possible parameters (see Synthesis section). These reactions suggest that the chainlike form in compound **2** is thermodynamically more stable compared to the dimeric form along with lattice $H_4L$ in compound **1**. When the temperature is increased from 150 to 200 °C, the yield of **2** increases and in the temperature in region 170−200 °C only compound **2** is formed as pure block crystals. The crystallization of compound **1** was observed in the temperature range 150−160 °C. The temperature dependent crystallization of the products formed in the present study has been described in the section of Supporting Information. The initial acidic pH (1.90) of the reaction mixture is responsible for the existence of protonated form ($H_4L$) of the ligand as a lattice component. As shown in Scheme 3, the phosphonic acid $H_4L$ (shown in red), which remains as a lattice component in **1**, undergoes deprotonation resulting in $H_2L$ which bridges two copper centers in compound **2**. The coordinated/deprotonated $H_2L$, present in compound **1**, gets protonated to $H_3L$ in the formation of **2**. Thus compound **1** can be considered as an intermediate in the formation of compound **2** since both have identical chemical compositions and also compound **1** could not be isolated at a higher temperature indicating it to be thermodynamically a less stable phase at higher temperature. Detailed mechanisms for the formation of compounds **1** and **2** are given in the following equations.

$$CuSO_4\cdot 5H_2O + 2,2'\text{-bpy} + H_4L \xrightarrow[\text{pH=1.90}]{180^\circ C} [Cu(2,2'\text{-bpy})(H_3L)(H_2L)]_2\cdot 2H_2O\ (\mathbf{2})$$

$$CuSO_4\cdot 5H_2O \xrightarrow{H_2O} [Cu(H_2O)_6]^{2+}SO_4^{2-}$$

$$[Cu(H_2O)_6]^{2+}SO_4^{2-} + 2,2'\text{-bpy} \xrightarrow{120^\circ C} [Cu(2,2'\text{-bpy})(H_2O)_2SO_4]_n\ (\mathbf{1A})$$

$$[Cu(2,2'\text{-bpy})(H_2O)_2SO_4]_n + H_4L \xrightarrow[\text{pH=1.90}]{150^\circ C} [Cu(2,2'\text{-bpy})(H_2L)]_2\cdot H_4L\cdot 4H_2O\ (\mathbf{1}) + [Cu(2,2'\text{-bpy})(H_3L)(H_2L)]_2\cdot 2H_2O\ (\mathbf{2})$$


dx.doi.org/10.1021/cg3011162 | *Cryst. Growth Des.* 2012, 12, 5579−5597

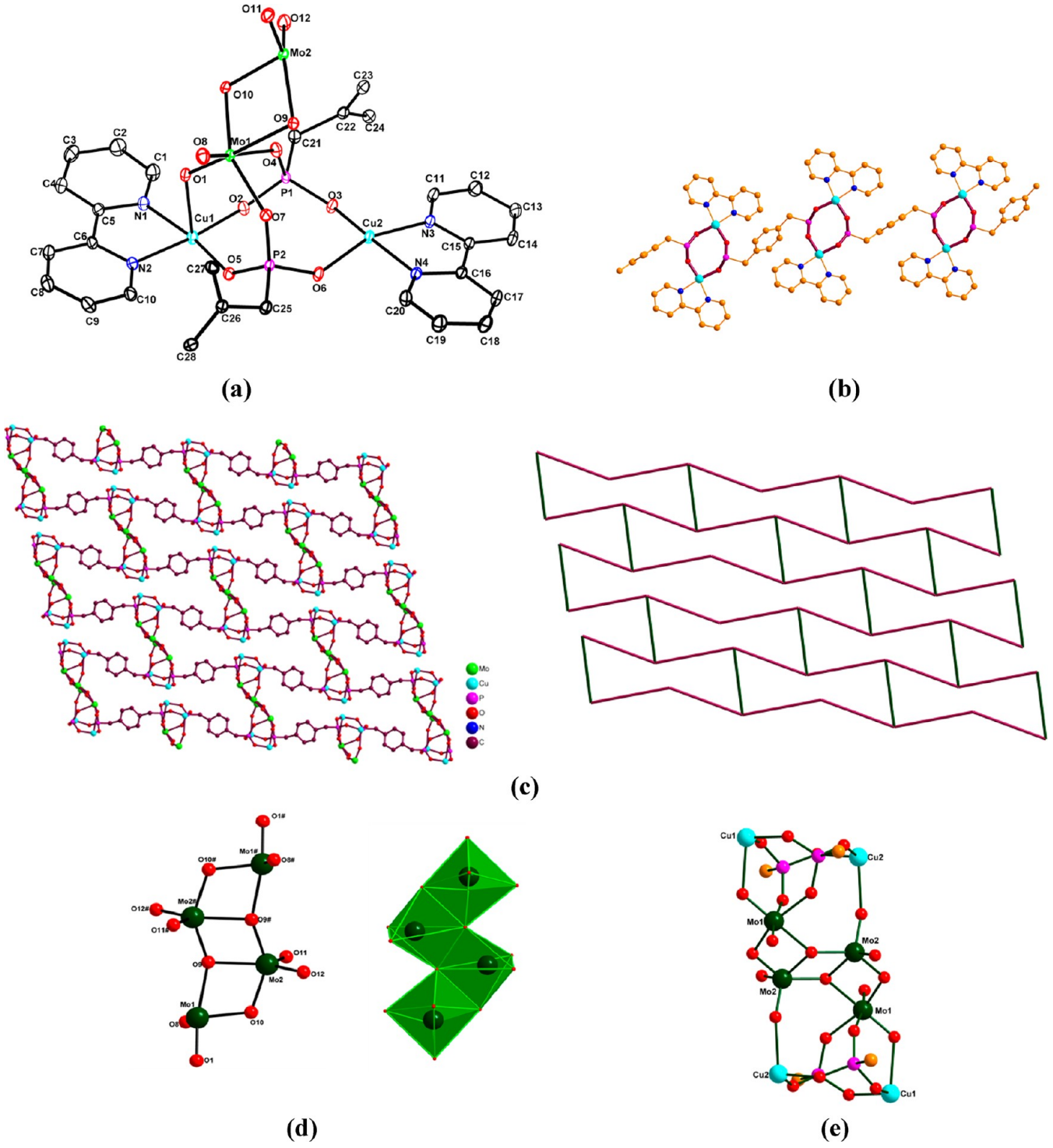


**Figure 6.** (a) ORTEP view of the basic unit of **6**. Hydrogen atoms and lattice water molecules have been removed for clarity. Thermal ellipsoids are at the 30% probability level. (b) 1D Cu-dimer chains formed by bridging $H_2L$ ligands. (c) 2D coordination polymer of the compound **6** and its topological representation (green color line indicates the $Mo_4O_{12}$ subunit). (d) Ball and stick, and polyhedral representations of the $Mo_4O_{12}$ subunit. (e) Panel showing the sandwiching of tetramolybdate between two Cu-dimers.

$$[Cu(2,2'\text{-bpy})(H_2O)_2SO_4]_n + H_4L \xrightarrow[pH=1.90]{180\,^{\circ}C} [Cu(2,2'\text{-bpy})(H_3L)(H_2L)]_2\cdot 2H_2O\ (\mathbf{2})$$

The compound **3** was isolated by employing 1,10-phenanthroline as coligand, and the single crystal X-ray analysis of compound **3** reveals the presence of Cu-dimeric unit similar to that found in compound **1**. The compound **3** was obtained as a single major product in the temperature region of 150−180 °C. Compound **3** was also formed starting from **3A** as explained in the case of **1**. The stability of compound **3** in comparison to compound **1** can be attributed to the absence of lattice $H_4L$ ligand. The initial pH of the reaction mixture in the formation of compound **3** was 2.50 in comparison to the pH of


dx.doi.org/10.1021/cg3011162 | *Cryst. Growth Des.* 2012, 12, 5579−5597

**Scheme 3**

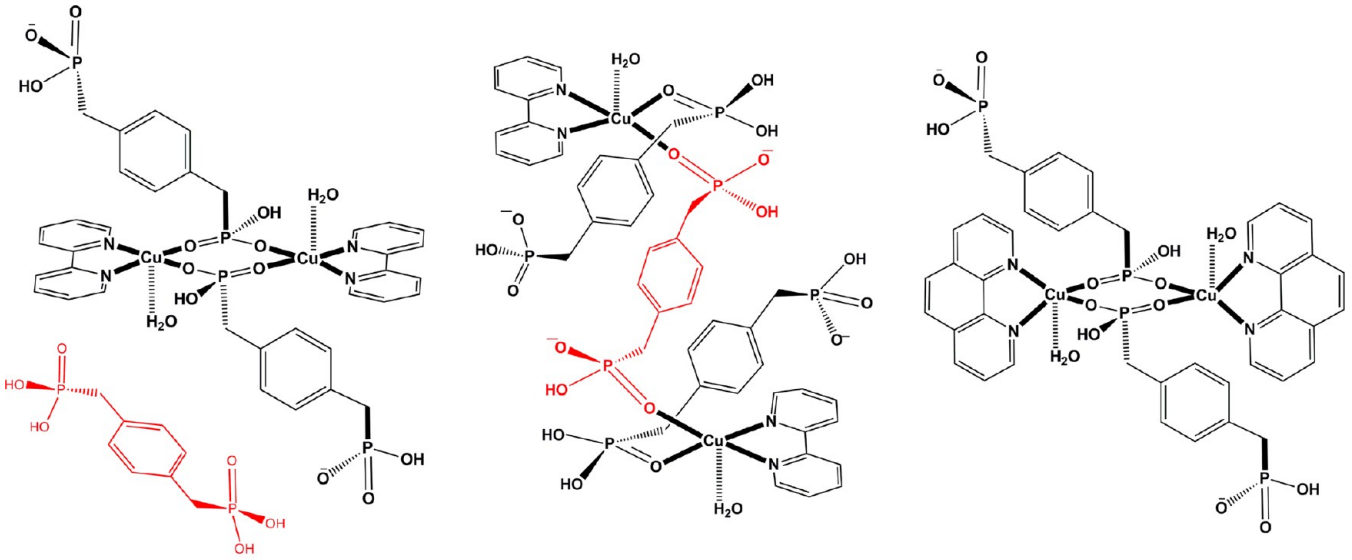


1.90 in the synthesis of the 2,2′-bpy system. The relatively higher pH of the reaction mixture in the synthesis of phenanthroline system might not favor the stabilization of $H_4L$ and $H_3L$ that are found in compounds **1** and **2**. The pH variation caused by the replacement of 2,2′-bpy with the 1,10-phenanthroline coligand limits the deprotonation to $H_2L$ thereby forming the dimeric compound **3**.

$$[Cu(H_2O)_6]^{2+}SO_4^{2-} + \text{1,10-phen} \xrightarrow[pH=2.5]{120^\circ C} [Cu(\text{1,10-phen})(H_2O)_2SO_4]_n \ (\mathbf{3A})$$

$$[Cu(\text{1,10-phen})(H_2O)_2SO_4]_n + H_4L \xrightarrow[pH=2.5]{150^\circ C} [Cu(H_2O)(\text{1,10-phen})(H_2L)]_2\cdot 6H_2O \ (\mathbf{3})$$

The O−P−O bridging in Cu-dimeric unit in compounds **1** and **3** is known to transmit weak to moderately strong antiferromagnetic and ferromagnetic exchange interactions efficiently between the two copper(II) ions. The extended structures with higher dimensionality, based on copper phosphonic acid dimeric systems, have been isolated at a relatively higher pH as compounds **4** and **5** (shown below). These two compounds represent the extension of the Cu-dimers by organic linkers. A temperature dependent hydrothermal synthesis reveals

$$CuSO_4\cdot 5H_2O + \text{2,2′-bpy} + H_4L \xrightarrow[pH=3.0]{180^\circ C} [Cu(\text{2,2′-bpy})H_2L]_n\cdot nH_2O \ (\mathbf{4})$$

$$CuSO_4\cdot 5H_2O + \text{1,10-phen} + H_4L \xrightarrow[pH=4.0]{180^\circ C} [Cu(\text{1,10-phen})H_2L]_n\cdot 3nH_2O \ (\mathbf{5})$$

that compounds **4** and **5** are also formed starting from the **1A** and **3A** respectively. For further investigations to obtain higher dimensional Cu-dimer systems, we have employed a molybdate based inorganic linker. Sodium molybdate undergoes hydrolysis to form molybdates of different nuclearities such as $MoO_4^{2-}$, $Mo_2O_7^{2-}$, $Mo_2O_3$, $Mo_4O_{12}$, $Mo_8O_{26}^{4-}$, etc.[34] depending on the pH of the reaction mixture and geometry of available coordination sites of the secondary metal, etc. The tetramolybdate $Mo_4O_{12}$, formed from $MoO_4^{2-}$, extends the dimensionality of Cu-dimer to 2D coordination polymer. The Cu···Cu separation is found to be 12.54 Å in compound **6** (tetramolybdate is the linker) and that found in compounds **4** and **5** is 12.93 Å ($H_2L$ as a linker) (Figure 7).

$$CuSO_4\cdot 5H_2O + \text{2,2′-bpy} + Na_2MoO_4 + H_4L \xrightarrow[pH=6.1]{180^\circ C} [\{Cu(\text{2,2′-bpy})(MoO_3)\}_2(L)]_n\cdot 2nH_2O \ (\mathbf{6})$$

$$Na_2MoO_4 \xrightarrow{H_2O} MoO_4^{2-} + 2Na^+$$

$$4MoO_4^{2-} + 8H^+ \rightarrow Mo_4O_{12} + 4H_2O$$

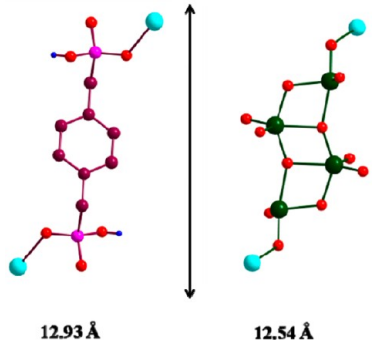


**Figure 7.** Length of the $H_2L$ and $Mo_4O_{12}$ subunits connecting the Cu-dimer chains.

The overall synthetic procedures for the formation compounds **1**−**6** representing the reaction parameters and conditions are shown in Scheme 4. The detailed protonation states of the phosphonic acid along with the secondary linkers are shown in Table 4.

**Thermogravimetric Studies (TGA).** TGA studies were carried out under the flow of $N_2$ for crystalline compounds **2**−**6**


dx.doi.org/10.1021/cg3011162 | *Cryst. Growth Des.* 2012, 12, 5579−5597

Scheme 4

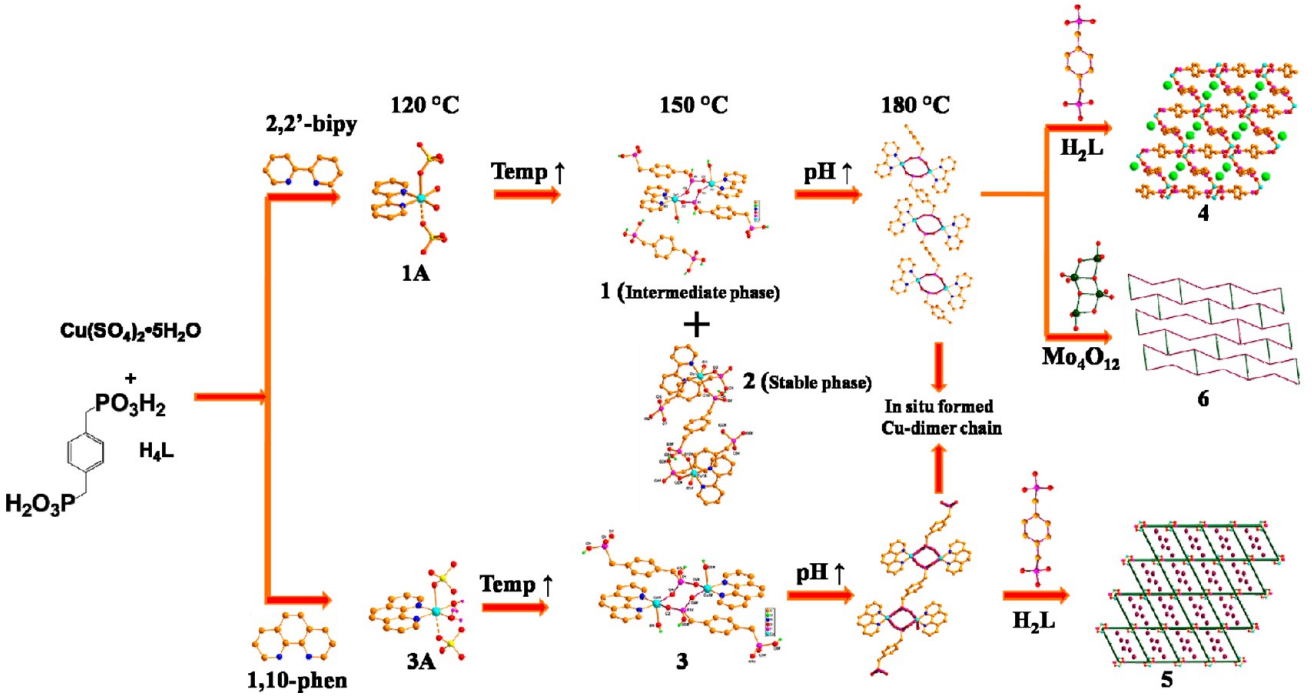


Table 4. Protonation State of the $H_4L$ with pH Value of the Reaction Mixture and Secondary Linker in the Compounds 1−6

| c. no. | secondary linker | pH | state of phosphonic acid |
|---|---|---|---|
| 1 | 2,2′-bpy | 1.90 | $H_4L$, $H_2L$ |
| 2 | 2,2′-bpy | 1.90 | $H_3L$, $H_2L$ |
| 3 | 1,10-phen | 2.5 | $H_2L$ |
| 4 | 2,2′-bpy | 3.0 | $H_2L$ |
| 5 | 1,10-phen | 4.0 | $H_2L$ |
| 6 | 2,2′-bpy | 6.1 | L |

in the temperature range 30−1000 °C. Compound **2** shows a continuous weight loss of 4.92% (calcd, 5.5%) from room temperature to 190 °C followed by decomposition in two steps with a residual mass of 32%. Compound **3** shows a weight loss of 10.21% at 170 °C corresponding to the loss of six water molecules (calcd, 12.41%), and the dimeric components remain stable up to 270 °C. Compound **3** decomposes in two steps at temperatures greater than 270 °C leaving behind the final residue of 40%. Compound **4** remains exceptionally stable up to 330 °C with a weight loss 4.02% (calcd, 3.5%) corresponding to the two lattice water molecules, and decomposition took place in two steps leaving a residue of 27.4%. The compound **5** contains six lattice water molecules and these water molecules are lost at 120 °C with a weight loss of 8.02% (calcd, 9.62%) and the relevant structure remains stable up to 325 °C. In the first step of its decomposition, the xylylene moieties come out with a weight loss of 19.84% (calcd, 18.89%) in the temperature range of 326−512 °C. In the second step, 1,10-phenanthroline moieties are eliminated in the temperature range of 520−1050 °C leaving a residue of 37.3%. The final product is estimated to be $Cu(PO_3)_2$ with a formula weight of 221.49 (39.2%). The thermogravimetric study of compound **5** reveals that the decomposition pattern follows the initial dehydration of lattice water molecules followed by the pyrolysis of organic units, leaving end product $Cu(PO_3)_2$. Compound **6** shows thermal stability up to 340 °C with initial dehydration of two water molecules of crystallization. The pyrolysis of organic units starts in the region of 350−800 °C leaving the final residue of 47.40% which is supposed to be $CuMoO_4$, $MoO_3$, $P_2O_5$.[35] The overall process of decomposition of **6** is consistent with the following equations.

$$[\{Cu(2,2'\text{-bpy})(MoO_3)\}_2(L)]\cdot 2H_2O \xrightarrow{30-180\,^\circ C} [\{Cu(2,2'\text{-bpy})(MoO_3)\}_2(L)]_n + 2H_2O$$

$$[\{Cu(2,2'\text{-bpy})(MoO_3)\}_2(L)] + 44O_2 \xrightarrow{350-800\,^\circ C} CuMoO_4 + MoO_3 + P_2O_5 + 28CO_2 + 4NO_2 + 12H_2O$$

Thermogravimetric curves of the compounds are shown in Figure 8 and the individual thermograms of the compounds are shown in the Supporting Information.

**PXRD Studies.** To ensure the phase purity of the products, X-ray powder diffraction studies for all the compounds have been performed and compared to the simulated diffraction patterns obtained from single crystal X-ray analysis. The similarity between observed and simulated patterns proves the bulk homogeneity of the crystalline solids (see Supporting Information for the PXRD patterns of the compounds **2**−**6**). Although the experimental patterns have very few unindexed diffraction peaks and some are slightly broadened and shifted in comparison to those simulated from the single-crystal data, it can still be regarded that the bulk synthesized materials have homogeneous phase.

**Variable Temperature PXRD Studies.** The TGA studies show that all the compounds are stable up to 300−350 °C. Variable temperature PXRD studies have been performed to ensure the stability of the frameworks of compounds **4** and **5** after the removal of lattice water molecules. The PXRD patterns of the dehydrated frameworks at different temper-


dx.doi.org/10.1021/cg3011162 | Cryst. Growth Des. 2012, 12, 5579−5597

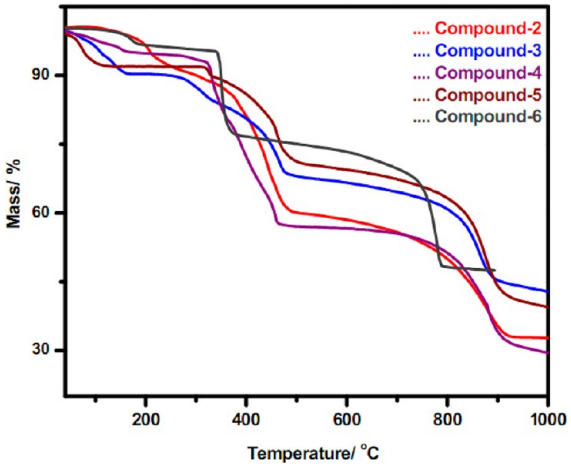


**Figure 8.** Thermogravimetric curves of compounds **2**–**6**.

atures show sharp peaks with almost same Bragg intensity. Some differences in the intensities of the reflections are observed at relatively higher temperatures due to the gradual loss of solvent water molecules. The TGA curve of compound **4** shows loss of lattice water molecules taking place at 170 °C. The VT-PXRD graphs of compound **4** are similar to the simulated pattern up to 130 °C and at 150 °C a new peak is observed in the region of 11.46° along with all the peaks displayed in the simulated pattern. At 170 °C, the intensity of the peak at 11.46° increases and the intensity of the peak corresponding to the reflection $(1\bar{1}0)$ at 12.35° is decreased and at 190 °C there is no peak corresponding to the $(1\bar{1}0)$ reflection. The slight shifting of the peak corresponding to the reflection $(1\bar{1}0)$ from 12.35° to 11.46° in the temperature region 150 to 190 °C indicates the expansion of the coordination network after losing the lattice water molecules. The powder pattern displayed at 190 °C is stable up to temperature 310 °C. These data indicate that crystals of coordination polymer **4** exhibit breathing-like behavior and the breathing starts at 150 °C. The dehydrated form of compound **4**, obtained by heating up to 170 °C, on exposure to the open atmosphere/water vapor at room temperature for 48 h results in the regeneration of original compound **4**. The regenerated PXRD pattern of the compound **4** shows similar peaks but the broadening of the peaks indicates the loss of crystallinity at higher temperatures (Figure 9). In compound **5**, lattice water molecules depart from the crystal in the temperature range of room temperature to 100 °C. The VT−PXRD pattern shows similar peaks displayed in the simulated pattern up to 310 °C with slight broadening of peak positions and the difference in the intensity of the peaks is due to loosely held water molecules in the lattice voids. The only major difference is the intensity of the peak corresponding to the reflection $(1\bar{1}0)$, which is decreased to a little extent at 50 °C and not at all appeared in the temperature range 70−310 °C. Unlike in compound **4**, no major shift of the peaks to the lower $2\theta$ values is observed in compound **5**. But when the dehydrated sample (obtained by heating at 70 °C) is taken and exposed to open atmosphere/water vapor at room temperature, it results in the incorporation of the lattice water molecules into the void spaces. An attempt to study the dehydration−rehydration cycle through single crystal to single crystal transformation was not successful due to the cracking of the crystals on heating. The results indicate that the compounds **4** and **5** have the potential to perform host−guest chemistry in the lattice voids. The relevant PXRD patterns (dehydration/rehydration) for compound **4** is shown in Figure 9 and for compound **5**, it is shown in the section of Supporting Information.

**Magnetic Behavior.** *Compound 3.* Variable temperature magnetic susceptibility measurements of a polycrystalline sample **3** have been performed at 2000 Oe between 2 and 300 K. The data are presented as a $\chi_M$ vs $T$ and $\chi_M T$ vs $T$ plots in Figure 10a (where $\chi_M$ is the molar magnetic susceptibility per $Cu^{II}_2$ unit). The room temperature (300 K) $\chi_M T$ product amounts to 0.78 $cm^3$ K $mol^{-1}$, which is in agreement with two uncoupled $S$ = 1/2 Cu(II) spins with unquenched orbital momentum ($\chi_M T$ = 0.375 $cm^3$ K $mol^{-1}$ for a $S$ = 1/2 ion). As the temperature is lowered, the $\chi_M T$ value continuously decreases to 0.68 $cm^3$ K $mol^{-1}$ at 65 K and then sharply decreases up to 2 K reaching a minimum value of 0.01 $cm^3$ K

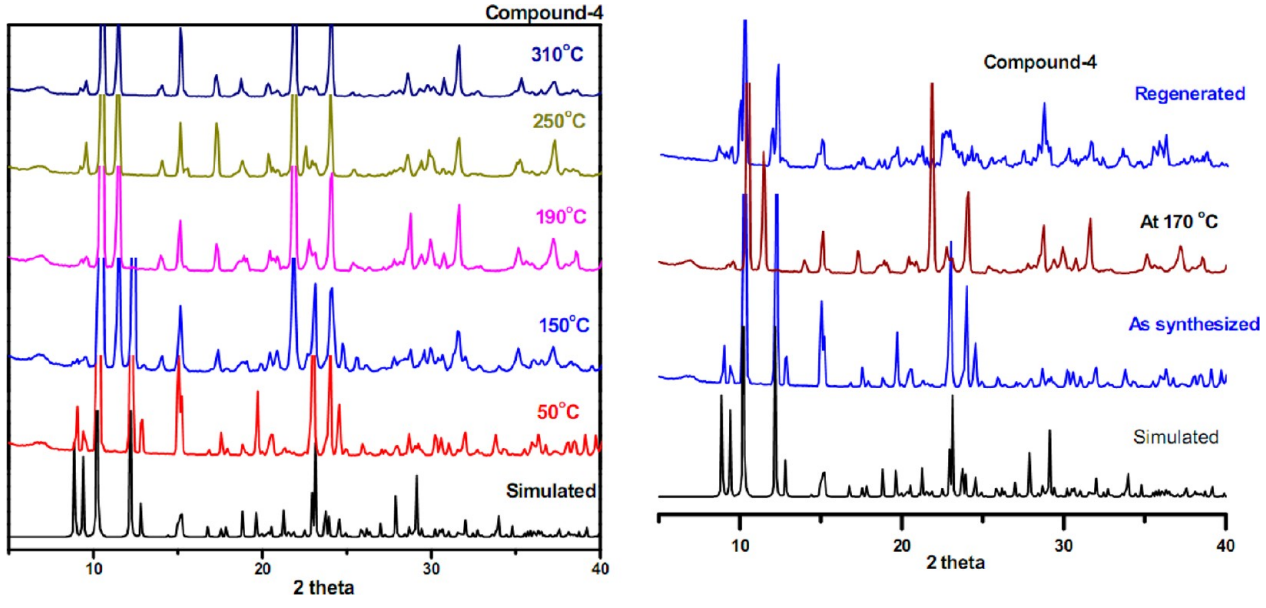


**Figure 9.** Variable temperature PXRD of the compound **4** representing the dehydration (left) and rehydration (right) of the lattice molecules.


dx.doi.org/10.1021/cg3011162 | *Cryst. Growth Des.* 2012, 12, 5579−5597

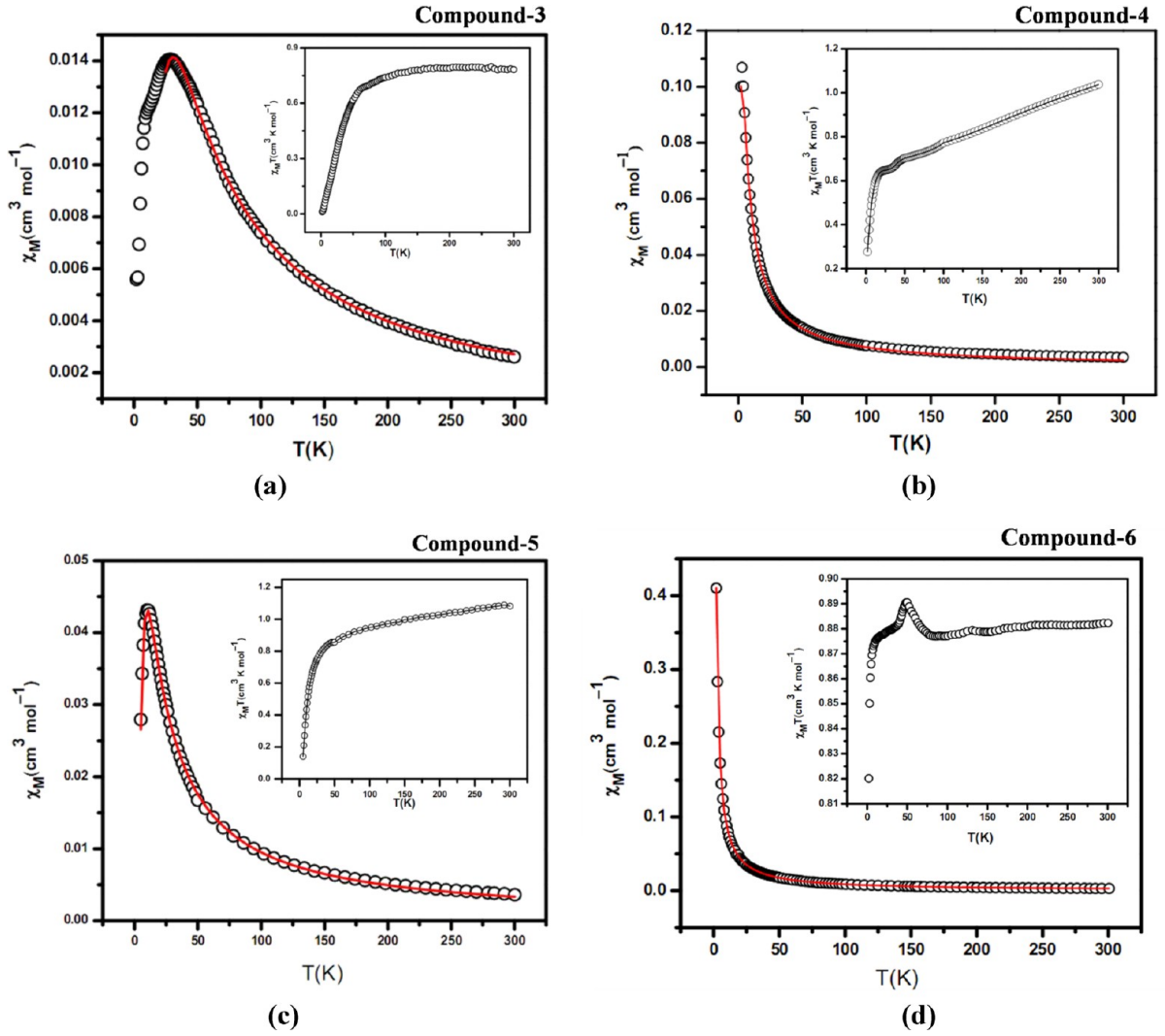


**Figure 10.** (a–d) Plots of $\chi_M$ vs $T$ and $\chi_M T$ vs $T$ (inset) for the compounds **3**, **4**, **5**, and **6** in the temperature range of 2–300 K. The red line indicates the fitting using theoretical model (see text).

$mol^{-1}$. The $1/\chi_M$ vs $T$ plot above the 50 K follows the Curie–Weiss law with negative Weiss constant $\theta = -16.7$ K. This magnetic behavior is generally observed for complexes that possess an intracomplex antiferromagnetic interaction. The magnetic interaction through the −O−P−O− bridges between two Cu(II) centers leads to a $S = 0$ ground state. A simple reasonable fit can be obtained for interacting dinuclear unit with conventional Hamiltonian: $H = -JS_1 \bullet S_2$ (where $S_1$ and $S_2$ are the spin operators with $S_1 = S_2 = 1/2$). Introducing an intercluster $zJ'$ term, the analysis of experimental values has been performed by the following expression:

$$\chi_M = \chi_M'/\{1 - \chi_M'(2zJ'/Ng^2\beta^2)\}$$

where $\chi_M' = 2Ng^2\beta^2/kT[3 + \exp(-J/kT)]$.

The values giving the best fit are $J = -36.44(1)$ $cm^{-1}$, $zJ' = +3.99(3)$ $cm^{-1}$ and $g = 2.100(4)$ [$R = 3.2 \times 10^{-4}$].

*Compound 4.* Compound **4** is 2D coordination polymer constituted by Cu dimers bridged by phosphonic acid as the nodes and *p*-xylylenediphosphonic acid as linker. The main structural difference between the discrete dimer (e.g., compounds **1** and 3) and the dimer present in coordination polymer **4** can be described by the apical site, which, in the discrete dimer, is occupied by the oxygen atom from the aqua ligand and in coordination (polymer) dimer is coordinated by phosphonate oxygen. Figure 10b shows the temperature dependence of $\chi_M$ and $\chi_M T$ values for compound **4.** The room temperature $\chi_M T = 1.03$ $cm^3$ K $mol^{-1}$ is higher than the expected value for two uncoupled $Cu^{II}$ ions. The $\chi_M T$ value gradually decreases upon cooling and reaches a minimum value 0.63 $cm^3$ K $mol^{-1}$ at 18 K and sharply decreases to 0.27 $cm^3$ K $mol^{-1}$ at 2 K. The $1/\chi_M$ vs $T$ plot above 30 K follows the Curie–Weiss law with negative Weiss constant with $\theta = -18.1$ K. The nature of the $\chi_M T$ vs $T$ plot and the negative Weiss constant suggest a dominant antiferromagnetic exchange between the two $Cu^{II}$ ions through the −O−P−O− bridges. The susceptibility data analyzed by the expression, described above, gives the best fit parameters, $J = -3.03(2)$ $cm^{-1}$, $zJ' = -0.88(5)$ $cm^{-1}$, and $g = 1.961(5)$ with an agreement factor $R = 7.2 \times 10^{-6}$, where $R = \Sigma[(\chi_M T)_{exp} - (\chi_M T)_{cal}]^2/\Sigma(\chi_M T)_{exp}^2$. From the values, obtained, the magnitude of exchange has been decreased in the case of dimer found in coordination polymer compared to that in discrete dimer.

*Compound 5.* Compound **5** is an extended coordination polymer of compound **3** in which 1,10-phenanthroline chelates the metal atoms. The plots of both $\chi_M$ vs $T$ and $\chi_M T$ vs $T$ per $Cu^{II}_2$ unit for compound **5** are shown in Figure 10c. Room


dx.doi.org/10.1021/cg3011162 | *Cryst. Growth Des.* 2012, 12, 5579–5597

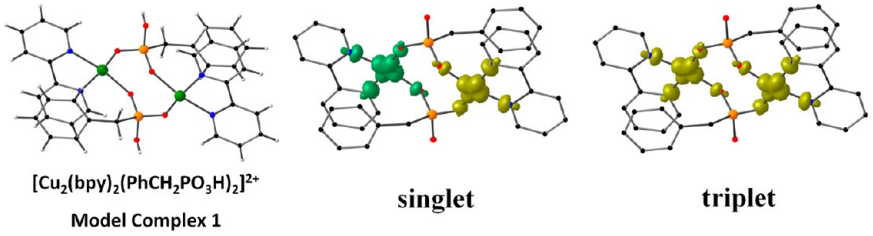


**Figure 11.** Spin density maps calculated for the two spin states of the model complex **1** (left) at B3LYP level for compound **1**. Positive and negative spin populations are represented as yellow and green surfaces. The isodensity surfaces correspond to a value of 0.01 e/$b^3$. Color code: green = Cu, orange = P, red = O, blue = N, black = C and light gray = H.

**Table 5. Magnetostructural Correlations (see also Scheme 4)**[a]

| c. no. | $d_{Cu-Cu}$ (Å) | conformation | $\tau_{avg1}/\tau_{avg2}$ (°) | $J$ ($cm^{-1}$) | $J_{DFT}$ ($cm^{-1}$) | ref |
|---|---|---|---|---|---|---|
| 1 | 5.12 | chair | 98.70/98.70 | | −13 | this work |
| 3 | 5.15 | chair | 99.32/99.32 | −36.44 | −51 | |
| 4 | 5.14 | chair | 102.4/102.4 | −3.03 | −68 | |
| 5 | 5.11 | chair | 99.18/99.18 | −11.8 | −45 | |
| 6 | 5.08 | crown | 95.31/99.74 | +1.14 | +4 | |
| | 5.17 | chair | 100.79/100.79 | −1.53 | | 20a |
| | 4.69 | chair | 73.02/73.02 | 1.86 | | 20b |
| | 4.73 | crown | 57.35/82.38 | −2.35 | | 16d |
| | 4.91 | crown | 72.06/91.76 | −0.23 | | 16d |

[a]Sign of the torsion angle was not considered when the values are averaged.

temperature (300K) $\chi_M T$ value of 1.08 $cm^3$ K $mol^{-1}$ is higher than the expected value for two uncoupled $Cu^{II}$ ions ($\chi_M T$ = 0.375 $cm^3$ K $mol^{-1}$ for a $S$ = 1/2 ion). As the temperature is lowered, the $\chi_M T$ decreases gradually to 0.80 $cm^3$ K $mol^{-1}$ at 30 K and then sharply decreases to minimum value of 0.13 $cm^3$ K $mol^{-1}$ at 5 K. $1/\chi_M$ vs $T$ plot above the 30 K follows the Curie–Weiss law with negative Weiss constant $\theta$= −19.2 K. The negative Weiss constant indicates the dominant antiferromagnetic exchange in intradimer through −O−P−O− bridges. The experimental susceptibility values are analyzed by the theoretical expression, described above, to give the best fit parameters. The obtained parameters are $J$ = −11.18(3) $cm^{-1}$, $zJ'$ = −2.58(1) $cm^{-1}$ and $g$ = 2.340(5) with an agreement factor of $R = 1.9 \times 10^{-5}$. The exchange magnitude in the coordination polymer dimer increases by replacing 2,2′-bipyridine with 1,10-phenanthroline.

*Compound* ***6***. Compound **6** is an extended coordination polymer of the discrete Cu-dimer which extends by the $Mo_4O_{12}$ subunit. The apical coordination site of the copper metal atom in this polymer is occupied by the oxygen atom from the $Mo_4O_{12}$ subunit. The plots of both $\chi_M$ vs $T$ and $\chi_M$T vs $T$ for **5** per $Cu^{II}_2$ unit are shown in Figure 10d. The $\chi_M T$ value at the room temperature is 0.88 $cm^3$ K $mol^{-1}$ which is slightly higher than the expected value of two uncoupled $Cu^{II}$ ions. Interestingly the decrease in the $\chi_M T$ value by lowering the temperature is very low. The $\chi_M T$ value is almost constant up to 70 K and then slightly increases to 0.89 $cm^3$ K $mol^{-1}$ and then decreases to minimum value of 0.82 $cm^3$ K $mol^{-1}$. $1/\chi_M$ vs $T$ plot above the 30 K follows the Curie–Weiss law with negligible negative Weiss constant $\theta$ = −0.1 K. This value indicates that there is no significant exchange between the two $Cu^{II}$ ions. To determine the magnitude of the exchange, the experimental susceptibilities are analyzed by the theoretical expression described above. The best fit parameters obtained were $J$ = −0.79(3) $cm^{-1}$, $zJ'$ = −0.16(1) $cm^{-1}$ and $g$ = 2.167 (1) with an agreement factor $R = 6.7 \times 10^{-7}$. By replacing the aqua ligand (in compounds **1** and **3**) and organic linker (compounds **4** and **5**) with the inorganic linker $Mo_4O_{12}$, the exchange through the −O−P−O− bridges was decreased drastically.

**Magnetostructural Correlations and DFT Studies.** To better understand the magnetic exchange mechanism in the reported complexes spin-unrestricted DFT calculations were performed on the complexes taking the geometries of the models from the crystal data (Figure 11). In the field of coordination polymers, the exchange interactions are generally calculated by using model structures that nearly resembles the basic repeating unit of the actual compound. We have considered dinuclear units for the compounds **3**, **4**, **5**, and **6** with slight variations from the actual ones as the model structures. Only the equatorial bonds are taken as bridges, as they interact directly with the magnetic orbitals on the Cu atoms d($x^2-y^2$). From Table 5, it is evident that the calculated $J$ values match with the experimental values only qualitatively (which is expected because in the actual complexes there are intercluster interactions), but the predicted sign of the exchange parameters is more important here (as the magnitudes are quite low), and matches satisfactorily. The variations in the $J$ values in the compounds are explained based on the two possible reasons.

*(a). Conformation of the Eight-Membered Cu-Dimer Rings.* The eight-membered Cu-dimer ring, formed in the compounds, can exist in 10 canonical conformations based on the torsion angles between the Cu−O−P−O atoms. The conformation of the ring has a vital role in the magnitude of the exchange between the two Cu(II) ions. In all the compounds, the bridging ligand occupies equatorial position at both Cu(II) ions ($O_{eq}$−P−$O_{eq}$). In compounds **2**, **3**, **4**, the ring exists in chair conformation and in compound **6** the ring exists in the crown conformation as shown in Figure 12. The Cu atoms in the dimers have a square pyramidal geometry in which the unpaired electron in the magnetic orbital on each copper atom is predominantly d($x^2-y^2$), the $x$ and $y$ axis being roughly defined by the copper to phosphonate oxygen bonds. These orbitals on Cu atoms are delocalized toward the 2p oxygen


dx.doi.org/10.1021/cg3011162 | *Cryst. Growth Des.* 2012, 12, 5579–5597

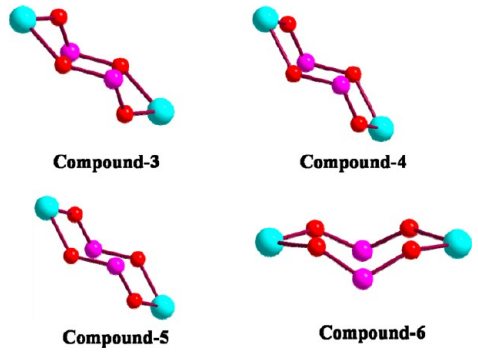


**Figure 12.** Conformations of the Cu-dimer rings present in the compounds **3**, **4**, **5**, and **6**.

orbitals of the O−P−O bridge and the exchange coupling through the phosphonate groups become operative. The overlap between the magnetic orbitals of the Cu(II) ion and the bridging oxygen atoms defines the pathway for the delocalization of the electron density between the metal centers. The conformation of the dimer ring can be explained based on the torsion angles between the Cu−O−P−O atoms. The eight-membered Cu-dimer can be explained by considering four types of torsion angle as shown in Scheme 5. The

**Scheme 5**

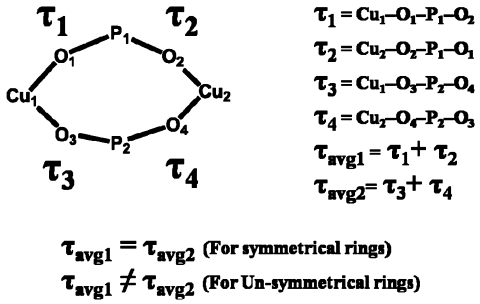


average of the torsion angles along the same bridges is represented by $\tau_{avg1}$ $\tau_{avg2}$. In symmetrical Cu-dimers $\tau_{avg1} = \tau_{avg2}$ and in unsymmetrical Cu-dimers these values are not equal to each other. Torsion angle explains the deviation of the phosphonate group from the mean Cu−O plane in the Cu−O−P−O−Cu skeleton, which accounts for the electron density delocalization pathways between the metal centers. Doyel et al. reported a series of copper complexes with pyrophosphate bridges in which the slight structural differences concerning the Cu−O−P−O−Cu skeleton are measured by the angles P−O−Cu angle $\alpha$ and the angle $\delta$ between the O−P−O plane and Cu−O axis.[36] For the large $\delta$ values the main delocalization from the metal ion to the bridge occurs through a $\pi$ pathway leading to strong antiferromagnetic contributions. A simple discrete Cu-dimer bridged by the pyrophosphate unit was reported by the Kruger in which the overlap between the magnetic orbitals of the two Cu (II) ions are predicted to be $\sigma$ exchange pathways as a result weak magnetic coupling, that is expected with the $J$ values −20 $cm^{-1}$.[37] As shown in the Table 5, $\tau_{avg}$ values for the chair conformations are more when compared to the crown conformation. A linear relationship is observed between the $J_{DFT}$ values and $\tau_{avg}$ values in the compounds **1**, **3**, **4**, **5**, and **6**. It is also interesting to note that for compound **6**, which has the crown conformation, the predicted $J$ value is very low and positive, matching nicely with the experimental results.

In compound **6**, the two Cu atoms are bridged differently by the O−P−O moieties in the crown conformation which enables the $\tau_{avg}$ to go below the critical limit stabilizing the triplet state making the exchange parameter positive. Only a few three atom phosphonate bridged Cu(II) complexes are available for comparison. Chandrasekhar et al. reported simple discrete phosphonate bridged copper complex[20a] $[Cu_2(\mu_2\text{-}C_3H_7PO_3)_2(bpya)_2(H_2O)_2]\cdot(H_2O)_2$ in which the $J$ value is −1.53 $cm^{-1}$ with $\tau_{avg}$ value 100.5°. In contrast Zurowska found a weak ferromagnetic interaction between the two metal centers in the compound $Cu_2(2\text{-mpmpe})_2(H_2O)_2(NO_3)_2$ with $J$ = 1.86 $cm^{-1}$ in which $\tau_{avg}$ is 72.5°.[20b] Also Chandrasekhar reported a series of hexanuclear compounds[16d] in which the Cu-dimers bridged by phosphonic acids are linked by the oxo-bridged Cu-dimer. The magnetic exchange in these compounds is mainly due to Cu(II) ions bridged by oxo groups only. The weak antiferromagnetic exchange is observed between the Cu(II) ions bridged by the phosphonic acid group with $J$ values in the range of −0.23 to −2.35 $cm^{-1}$ in which the $\tau_{avg}$ values are in the range of 50° to 85°. In the phosphonate bridged Cu(II) complexes, if the $\tau_{avg}$ values are below 100° then weak antiferromagnetic and ferromagnetic interactions are observed between Cu(II) ions; if $\tau_{avg}$ value is more than 100°, then a moderate to strong antiferromagnetic interactions are observed between the Cu(II) ions. Even though this factor is important in determining the magnitude of the exchange parameter, additional factors are also needed to fully account the variations in the exchange parameters, e.g., electronic effect induced by the atoms connected to the oxygen atom which are not part of the dimer.

*(b). Electronic Effect Induced by the Peripheral Subunits.* In the phosphonate bridge, the oxygen atom which is protonated and noncoordinated in compounds **3**, **4**, and **5** is deprotonated and coordinated to the large electron withdrawing group $Mo_4O_{12}$ in the compound **6**, which exerts the electron withdrawing effect on the bridging atoms, thereby decreasing the electron density on the oxygen atoms. This causes a small overlap between the metal magnetic orbitals through the bridge resulting in the exchange to be very weak. Doyel shows the effect of protonation of noncoordinated oxygen atom on the exchange parameter in the pyrophosphate mediated magnetic interactions in Cu(II) coordination complexes.[36]

## CONCLUSION

In summary we report here the six new coordination polymers (**1**−**6**) based on the simple building unit Cu-dimer bridged by *p*-xylylenediphosphonic acid and secondary chelated linkers (2,2′-bpy, 1,10-phen). We have explored the coordination chemistry of eight-membered Cu-dimer ring, in which the terminal sites are chelated by secondary linkers, as SBUs in construction of multidimensional coordination architectures. The mechanisms for the formation of Cu-dimer starting from **1A** to **1** and **2**, **3A** to **3** have been investigated with varying the temperature. Compounds **1**−**3** represents the classical example in which the pH, induced by the secondary linker, changes composition of the structure. Compounds **4** and **5** represent the 2D architectures of the Cu-dimer extended by the organic linker $H_2L$ in which the dimer acts as a node and $H_2L$ ligands as linkers. The large void spaces in the (4, 4) connected nets of **4** and **5** can be potentially used for the host−guest phenomenon


dx.doi.org/10.1021/cg3011162 | Cryst. Growth Des. 2012, 12, 5579−5597

which has been proved by the dehydration−rehydration of the lattice water molecules. Compound **6** represents the 2D coordination polymer of the dimer which is extended by the inorganic linker $Mo_4O_{12}$. All the compounds are thermally stable up to the temperature region 350 °C. The OPO bridges in the eight-membered Cu-dimer rings show net antiferromagnetic interactions between the Cu(II) ions in the compounds **3**, **4**, **5** and **6**. DFT calculations correlates the magnitude of the exchange parameter with the conformation of the eight-membered ring based on the torsion angles of the conformation that reveals the electron density delocalization pathways between the two $Cu^{II}$ ions through OPO bridges. By changing the linkers (organic and inorganic), the conformation can be tuned which enhances the magnetic exchange between the metal centers. In short this article gives a comprehensive study of the new class of SBU (Cu-dimer bridged by phosphonic acid) in metal phosphonate chemistry in prospects of formation and stabilization in a coordination matrix, which gives an opportunity to construct the coordination polymers with potential void spaces and finally temperature dependent magnetic exchange phenomenon through phosphonate bridges. We are presently working on exploration of this SBU with various linkers to design the materials with functional applications.

## ■ ASSOCIATED CONTENT

### Supporting Information

Crystallographic information files; powder X-ray patterns and thermogravimetric curves of compounds **2**−**6**; variable temperature PXRD of compounds **4** and **5**; $1/\chi_M$ vs $T$ plots of compounds **3**−**6**; ORTEP diagrams of compounds **1**−**3**; spin density maps calculated for the two spin states of the model complexes **3**−**6**; table showing the formation of different phases by varying the temperature; crystal data and structural refinement parameters for compounds **1A** and **3A**; selected bond lengths and bond angles of the compounds **1**−**6**. This material is available free of charge via the Internet at http://pubs.acs.org.

## ■ AUTHOR INFORMATION

### Corresponding Author

*E-mail: skdsc@uohyd.ernet.in; samar439@gmail.com. Fax: +91-40-2301-2460. Tel: +91-40-2301-1007.

### Notes

The authors declare no competing financial interest.

## ■ ACKNOWLEDGMENTS

The authors thank the Department of Science and Technology, Government of India (Project No. SR/SI/IC-23/2007) and Centre for Nanotechnology (CFN), University of Hyderabad for financial support. The National X-ray Diffractometer facility at University of Hyderabad by the Department of Science and Technology, Government of India, is gratefully acknowledged. We are grateful to UGC, New Delhi, for providing the infrastructure facility at University of Hyderabad under UPE grant. We thank Prof. S. N. Kaul (CFN) and his group members, especially Mr. Ravi helping in recording magnetic measurements. We thank Prof. P. S. Mukherjee (IISC) for helping us in the analysis of magnetic data. BKT and SM thank UGC and CSIR, Government of India, respectively, for their fellowships.

## ■ REFERENCES

(1) (a) Wang, B.; Cote, A. P.; Furukawa, H.; O'Keeffe, M.; Yaghi, O. M. *Nature* **2008**, *453*, 207. (b) Kitagawa, S.; Kitaura, R.; Noro, S. *Angew. Chem. Int. Ed.* **2004**, *43*, 2334. (c) Chen, X.-M.; Tong, M.-L. *Acc. Chem. Res.* **2007**, *40*, 162. (d) Zheng, B.; Dong, H.; Bai, J.; Li, Y.; Li, S.; Scheer, M. *J. Am. Chem. Soc.* **2008**, *130*, 7778. (e) Wang, X.-L.; Qin, C.; Wang, E.-B.; Xu, L.; Su, Z.-M.; Hu, C.-W. *Angew. Chem., Int. Ed.* **2004**, *43*, 5036. (f) Robson, R. *Dalton Trans.* **2008**, 5113. (g) Jiang, L.; Zhang, X.-B.; Han, S.; Xu, Q. *Inorg. Chem.* **2008**, *47*, 4826.

(2) (a) Kitura, R.; Fujimoto, K.; Noro, S.; Kondo, M; Kitagawo, S. *Angew. Chem., Int. Ed.* **2002**, *41*, 133. (b) Shin, D. M.; Lee, I. S.; Chung, Y. K. *Inorg. Chem.* **2003**, *42*, 8838. (c) Ayappan, P; Evans, O, R.; Cui, Y.; Wheeler, K. A.; Lin, W. B. *Inorg. Chem.* **2002**, *41*, 4978. (d) Dinca, M.; Long, J. R. *J. Am. Chem. Soc.* **2005**, *127*, 9376. (e) Yoon, J. W.; Jung, S. H; Hwang, Y. K.; Humphrey, S. M.; Wood, P. T.; Chang, J. S. *Adv. Mater.* **2007**, *19*, 1830. (f) Han, S. S.; Deng, W, Q.; Goddard, W. A. *Angew. Chem., Int. Ed.* **2007**, *46*, 6289. (g) Bar, A. K.; Chakrabarty, R.; Chi, K.-W.; Batten, S. R.; Mukherjee, P. S. *Dalton Trans.* **2009**, 3222.

(3) (a) Li, H.; Eddaoudi, M.; Groy, T. L.; Yaghi, O. M. *J. Am. Chem. Soc.* **1998**, *120*, 8571. (b) Chen, B.; Eddaoudi, M.; Hyde, S. T.; O'Keeffe, M.; Yaghi, O. M. *Science* **2001**, *291*, 1021. (c) Eddaoudi, M.; Kim, J.; Rosi, N.; Vodak, D.; Wachter, J.; O'Keeffe, M.; Yaghi, O. M. *Science* **2002**, *43*, 2334. (d) Yaghi, O. M.; O'Keeffe, M.; Ockwig, N.; Chae, H.; Eddaoudi, M.; Kim, J. *Nature* **2003**, *423*, 705.

(4) (a) Zhang, B.; Clearfield, A. *J. Am. Chem. Soc.* **1997**, *119*, 2751. (b) Alberti, G.; Lehn, J. M. *Comprehensive Supramolecular Chemistry*; Pergamon, Elsevier Science Ltd.: Oxford, UK, 1996, Vol. 7. (c) Cao, G.; Hong, H.; Mallouk, T. E. *Acc. Chem. Res.* **1992**, *25*, 420. (d) Maillet, C.; Janvier, P.; Pipelier, M.; Praveen, T.; Andres, Y.; Bujoli, B. *Chem. Mater.* **2001**, *13*, 2879. (e) Gomez, R.; Segura, J. L.; Martin, N. *J. Org. Chem.* **2000**, *65*, 7566. (f) Ungashe, S. B.; Wilson, W. L.; Katz, H. E.; Scheller, G. R.; Putvinski, T. M. *J. Am. Chem. Soc.* **1992**, *114*, 8717. (g) Tripuramallu, B. K.; Kishore, R.; Das, S. K. *Polyhedron* **2010**, *29*, 2985.

(5) (a) Mietrach, A.; Muesmann, T. W. T.; Christoffers, J.; Wickleder, M. S. *Eur. J. Inorg. Chem.* **2009**, 5328. (b) Yi, F. Y.; Lin, Q. P.; Zhou, T. H; Mao, J. G. *Cryst. Growth Des.* **2010**, *10*, 1788.

(6) (a) Lin, P.; Clegg, W.; Harrington, R. W.; Henderson, R. A. *Dalton Trans.* **2005**, 2388. (b) Dinca, M.; Long, J. R. *J. Am. Chem. Soc.* **2007**, *129*, 11172. (c) Pachfule, P.; Das, R.; Poddar, P.; Banerjee, R. *Cryst. Growth Des.* **2010**, *10*, 2475. (d) Li, Z. X.; Zeng, Y. F.; Ma, H.; Bu, X. H. *Chem. Commun.* **2010**, *46*, 8540. (e) Fan, J.; Yee., G. T.; Wang, G.; Hanson, B. E. *Inorg. Chem.* **2006**, *45*, 599. (f) Li, Z. X.; Xu, Y.; Zuo, Y.; Li, L.; Pan, Q.; Hu, T. L.; Bu, X. H. *Cryst. Growth Des.* **2009**, *9*, 3904. (g) Imaz, I.; Maspoch, D.; Blanco, C. R.; Falcon, J. M. P.; Campo, J.; Molina, D. R. *Angew. Chem., Int. Ed.* **2008**, *47*, 1857. (h) Yang, J.; Ma, J. F.; Batten, S. R.; Su, Z. M. *Chem. Commun.* **2008**, 2233. (i) Sathiyendiran, M.; Wu, J. Y.; Velayudham, M.; Lee, G. H.; Peng, S. M.; Lu, K. L. *Chem. Commun.* **2009**, 3795. (j) Su, C. Y.; Cai, Y. P.; Chen, C. L.; Smith, M. D.; Kaim, W.; ZurLoye, H. C. *J. Am. Chem. Soc.* **2003**, *125*, 8595. (k) Lan, Y. Q.; Li, S. L.; Qin, J. S.; Du, D. Y.; Wang, X. L.; Su, Z. M.; Fu, Q. *Inorg. Chem.* **2008**, 10600.

(7) (a) Collins, D. J.; Zhou, H.-C. *J. Mater. Chem.* **2007**, *17*, 3154. (b) James, S. L. *Chem. Soc. Rev.* **2003**, *32*, 705. (c) Millward, A. R.; Yaghi, O. M. *J. Am. Chem. Soc.* **2003**, *125*, 11490.

(8) (a) Maeda, K.; Kiyozumi, Y.; Mizukami, F. *J. Phys. Chem. B* **1997**, *101*, 4402. (b) Odobel, F.; Bujoli, B.; Massiot, D. *Chem. Mater.* **2001**, *13*, 163. (c) Alberti, G.; Casciola, M.; Costantino, U.; Peraio, A.; Montoneri, E. *Solid State Ionics* **1992**, *50*, 315. (d) Alberti, G.; Casciola, M. *Solid State Ionics* **1997**, *97*, 177. (e) Vermeulen, L. A.; Thompson, M. E. *Nature* **1992**, *358*, 656. (f) Deniaud, D.; Schollorn, B.; Mansuy, D.; Rouxel, J.; Battioni, P.; Bujoli, B. *Chem. Mater.* **1995**, *7*, 995.

(9) (a) Yin, P.; Gao, S.; Wang, Z -M.; Yan, C.-H.; Zheng, L.-M.; Xin, X.-Q. *Inorg. Chem.* **2005**, *44*, 2761. (b) Chandrasekhar, V.; Senapati, T.; Dey, A; Sanudo, E. C. *Inorg. Chem.* **2011**, *50*, 1420. (c) Hou, S.-Z.; Cao, D-K; Li, Y.-Z.; Zheng, L.-M. *Inorg. Chem.* **2008**, *47*, 10211.

(d) Papoutsakis, D.; Jackson, J. E.; Nocera, D. G. *Inorg. Chem.* **1996**, *35*, 800.
(10) Shimizu, G. K. H.; Vaidhyanathan, R.; Taylor, J. M. *Chem. Soc .Rev.* **2009**, *38*, 1430.
(11) (a) Quellette, W.; Yu, M. H.; O'Connor, C. J.; Zubieta. *J. Inorg. Chem.* **2006**, *45*, 3224. (b) Quellette, W.; YU, M. H.; O'Connor, C. J.; Zubieta. *J. Inorg. Chem.* **2006**, *45*, 7628.
(12) (a) Bolligarla, R.; Das, S. K. *CrystEngComm* **2010**, 3409. (b) Tripuramallu, B. K.; Kishore, R.; Das, S. K. *Inorg. Chim. Acta* **2011**, *368*, 132.
(13) (a) Tripuramallu, B. K.; Manna, P.; Reddy, S. N.; Das, S. K. *Cryst. Growth Des.* **2012**, *12*, 777. (b) Manna, P.; Tripuramallu, B. K.; Das, S. K. *Cryst. Growth Des.* **2012**, *12*, 4607.
(14) (a) Bakhmutova, E. V.; Ouyang, X.; Medvedev, D. G.; Clearfield, A. *Inorg. Chem.* **2003**, *42*, 7046. (b) Drumel, S.; Janvier, P.; Barboux, P.; Doeuff, M. B.; Bujoli, B. *Inorg. Chem.* **1995**, *34*, 148. (c) Bideau, J. L.; Payen, C.; Palvadeau, P.; Bujoli, B. *Inorg. Chem.* **1994**, *33*, 4885. (d) Song, S. Y.; Ma, J. F.; Yang, J.; Cao, M. H.; Zhang, H. J.; Wang, H. S.; Yang, K. Y. *Inorg. Chem.* **2006**, *45*, 1201. (e) Cao, G.; Lee, H.; Lynch, V. M.; Mallouk, T. E. *Inorg. Chem.* **1988**, *27*, 2781. (f) Clearfield, A.; Wang, Z. *J. Chem. Soc., Dalton Trans.* **2002**, 2937.
(15) (a) Mehring, M.; Schurmann, M. *Chem. Commun.* **2001**, 2354. (b) Baskar, V.; Shanmugam, M.; Sanudo, E. C.; Shanmugam, M.; Collison, D.; McInnes, E. J. L.; Wei, Q.; Winpenny, R. E. P. *Chem. Commun.* **2007**, 37. (c) Samanamu, C. R.; Olmstead, M. M.; Montchamp, J. L.; Richards, A. F. *Inorg. Chem.* **2008**, *47*, 3879. (d) Murugavel, R.; Shanmugan, S. *Chem. Commun.* **2007**, 1257.
(16) (a) Chandrasekhar, V.; Azhakar, R.; Senapati, T.; Thilagar, P.; Ghosh, S.; Verma, S.; Boomishankar, R.; Steiner, A.; T̈ogerle, P. *Dalton Trans.* **2008**, 1150. (b) Chandrasekhar, V.; Nagarajan, L.; Clérac, R.; Ghosh, S.; Verma, S. *Inorg. Chem.* **2008**, *47*, 1067. (c) Doyle, R. P.; Kruger, P. E.; Moubaraki, B.; Murray, K. S.; Nieuwenhuyzen, M. *Dalton Trans.* **2003**, 4230. (d) Chandrasekhar, V.; Senapati, T.; Sanudo, E. C. *Inorg. Chem.* **2008**, *47*, 9553.
(17) (a) Taylor, J. M.; Mahmoudkhani, A. M.; Shimizu, G. K. H. *Angew. Chem., Int. Ed.* **2007**, *46*, 795. (b) Kong, D.; Zon, J.; Clearfield, J. M. A. *Inorg. Chem.* **2006**, *45*, 977. (c) Vaidhyanathan, R.; Mahmoudkhani, A. H.; Shimizu, G. K. H. *Can. J. Chem.* **2009**, *87*, 247. (d) Evans, O. R.; Ngo, H. L.; Lin, W. *J. Am. Chem. Soc.* **2001**, *123*, 10395. (e) Liang, J.; Shimizu, G. K. H. *Inorg. Chem.* **2007**, *46*, 10449.
(18) (a) Almeida Paz, F. A.; Rocha, J.; Klinowski, J.; Trindade, T.; Shi, F.-N.; Mafra, L. *Prog. Solid State Chem.* **2005**, *33*, 113. (b) Lu, J. Y. *Coord. Chem. Rev.* **2003**, *246*, 327.
(19) (a) Perez, J.; Garcia, L.; Kessler, M.; Nolse, K.; Perez, E.; Serrano, J. L.; Martinez, J. F.; Carrascosa, R. *Inorg. Chim. Acta* **2005**, *358*, 2432. (b) Deng-Ke, C.; Jing, X.; Zhi, Y. L.; Modesto, C. J. J.; Eugenio, C.; Li-Min, Z. *Eur. J. Inorg. Chem.* **2006**, *9*, 1830. (c) Ling, S. J.; Gao, M. J. *Solid State Chem.* **2005**, *178*, 3514. (d) Gao, M. J.; Zhike, W.; Abraham, C. *Inorg. Chem.* **2002**, *41*, 3713. (e) Krassimira, G.; Rita, D.; Luis, L.; Michael, D.; Vitor, F. *Dalton Trans.* **2004**, *12*, 1812.
(20) (a) Chandrasekhar, V.; Senapati, T.; Clérac, R. *Eur. J. Inorg. Chem.* **2009**, 1640. (b) Zurowska, B.; Brzuszkiewicz, A.; Ochocki., J. *Polyhedron* **2008**, *27*, 1721.
(21) (a) Willet, R. D., Gattesdhi, D., Kahn, O., Eds. *Magneto-Structural Correlation in Exchange Coupled Systems*; Reidel: Dordrecht, 1985. (b) Carlin, R. L.; van Duyneveldt, A. J. *Magnetic Properties of Transition Metal Compounds*; Springer: Berlin, 1997.
(22) Mayer, C. R.; Herve, M.; Lavanant, H.; Blais, J. C.; Secheresse, F. *Eur. J. Inorg. Chem.* **2004**, *5*, 973.
(23) (a) Ruiz, E.; Alemany, P.; Alvarez, S.; Cano, J. *J. Am. Chem. Soc.* **1997**, *119*, 1297. (b) Ruiz, E.; Rodríguez-Fortea, A.; Cano, J.; Alvarez, S.; Alemany, P. *J. Comput. Chem.* **2003**, *24*, 982. (c) Ruiz, E.; Cano, J.; Alvarez, S.; Alemany, P. *J. Comput. Chem.* **1999**, *20*, 1391. (d) Ruiz, E. *Struct. Bonding (Berlin)* **2004**, *113*, 71.
(24) Becke, A. D. *J. Chem. Phys.* **1993**, *98*, 5648.
(25) Frisch, M. J.; Trucks, G. W.; Schlegel, H. B.; Scuseria, G. E.; Robb, M. A.; Cheeseman, J. R.; Montgomery, J. A.; Vreven, T.; Kudin, K. N.; Burant, J. C.; Millam, J. M.; Iyengar, S. S.; Tomasi, J.; Barone, V.; Mennucci, B.; Cossi, M.; Scalmani, G.; Rega, N.; Petersson, G. A.; Nakatsuji, H.; Hada, M.; Ehara, M.; Toyota, K.; Fukuda, R.; Hasegawa, J.; Ishida, H.; Nakajima, T.; Honda, Y.; Kitao, O.; Nakai, H.; Klene, M.; Li, X.; Knox, J. E.; Hratchian, H. P.; Cross, J. B.; Adamo, C.; Jaramillo, J.; Gomperts, R.; Stratmann, R. E.; Yazyev, O.; Austin, A. J.; Cammi, R.; Pomelli, C.; Ochterski, J.; Ayala, P. Y.; Morokuma, K.; Voth, G. A.; Salvador, P.; Dannenberg, J. J.; Zakrzewski, V. G.; Dapprich, S.; Daniels, A. D.; Strain, M. C.; Farkas, O.; Malick, D. K.; Rabuck, A. D.; Raghavachari, K.; Foresman, J. B.; Ortiz, J. V.; Cui, Q.; Baboul, A. G.; Clifford, S.; Cioslowski, J.; Stefanov, B. B.; Liu, G.; Liashenko, A.; Piskorz, P.; Komaromi, I.; Martin, R. L.; Fox, D. J.; Keith, T.; Al-Laham, M. A.; Peng, C. Y.; Nanayakkara,A.; Challacombe, M.; Gill, P. M. W.; Johnson, B.; Chen, W.; Wong, M. W.; Gonzalez, C.; Pople, J. A. *Gaussian 03*, revision B.4; Gaussian Inc.: Pittsburgh, PA, 2003.
(26) Becke, A. D. *Phys. Rev. A* **1988**, *38*, 3098.
(27) Lee, C.; Yang, W.; Parr, R. G. *Phys. Rev. B* **1988**, *37*, 785.
(28) Ruiz, E.; Alvarez, S.; Cano, J.; Polo, V. *J. Chem. Phys.* **2005**, *123*, 164110.
(29) (a) Mukherjee, S.; Gole, B.; Chakrabarty, R.; Mukherjee, P. S. *Inorg. Chem.* **2009**, *48*, 11325. (b) Mukherjee, S.; Gole, B.; Song, Y.; Mukherjee, P. S. *Inorg. Chem.* **2011**, *50*, 3621. (c) Mukherjee, S.; Patil, Y. P.; Mukherjee, P. S. *Dalton Trans.* **2012**, *41*, 54.
(30) (a) *SAINT: Software for the CCD Detector System*; Bruker Analytical X-ray Systems, Inc.: Madison, WI, 1998. (b) Sheldrick, G. M. *SADABS: Program for Absorption Correction*; University of Gottingen: Gottingen, Germany, 1997. (c) Sheldrick, G. M. *SHELXS-97: Program for Structure Solution*; University of Gottingen: Gottingen, Germany, 1997. (d) Sheldrick, G. M. *SHELXL-97: Program for Crystal Structure Analysis*; University of Gottingen: Gottingen, Germany, 1997.
(31) (a) Chattopadhyay, S. K.; Mak, T. C. W. *Inorg. Chem. Commun.* **2000**, *3*, 111. (b) Hu, X.; Guo, J.; Liu, C.; Zen, H.; Wang, Y.; Du, W. *Inorg. Chim. Acta* **2009**, *362*, 3421. (c) Zheng, Y.-Q.; Lin, J.−L. *Z. Anorg. Allg. Chem.* **2003**, *629*, 1622. (d) Dietz, C.; Seidel, R. W.; Oppel, I. M. *Z. Kristallogr.-New Cryst.Struct.* **2009**, *224*, 509.
(32) Cabeza, A.; Ouyang, X.; Sharma, C. V. K.; Aranda, M. A. G.; Bruque, S.; Clearfield, A. *Inorg. Chem.* **2002**, *41*, 2325.
(33) Jones, S.; Liu, H.; Schmidtke, K.; O'Connor, C. C.; Zubieta., J. *Inorg. Chem. Commun.* **2010**, *13*, 298.
(34) Pavani, K.; Ramanan, A. *Eur. J. Inorg. Chem.* **2005**, 3080.
(35) Armatas, N. G.; Allis, D. G.; Prosvirin, A.; Carnutu, G.; O'Connor, C. J.; Dunbar, K.; Zubieta, J. *Inorg. Chem.* **2008**, *47*, 832.
(36) Marino, N.; Ikotun, O. F.; Julve, M.; Lloret, F.; Cano, J.; Doyle, R. P. *Inorg. Chem.* **2011**, *50*, 378.
(37) Kruger, P. E.; Doyle, R. P.; Julve, M.; Lloret, F.; Nieuwenhuyzen, M. *Inorg. Chem.* **2001**, *40*, 1726.